

---

# Evaluation of markerless 3D joint position accuracy using high end vs. low end camera setups

---

Bachelor Thesis

by

**Kim Braunias**

born on 13.10.1992 in Düsseldorf

**Hochschule Koblenz, RheinAhrCampus**

**Fakultät für Mathematik und Technik**

Sportmedizinische Technik

Matrikel-Nr.: 522080

Supervisor:	Prof. Dr. Marco Junglas
Co-examiner	Prof. Dr. Ulrich Hartmann
Company advisor:	Dipl. Kfm Philipp Russ
Submission date:	27.05.2016
Done at:	Simi Reality Motion Systems GmbH Max-Planck-Str. 11 85705 Unterschleißheim

## Erklärung

Hiermit versichere ich, dass ich die vorliegende Arbeit selbständig und nur unter Verwendung der angegebenen Quellen und Hilfsmittel verfasst habe.

Zutreffendes bitte ankreuzen:

Mit der hochschulinternen Veröffentlichung der Arbeit bin ich

einverstanden       n i c h t einverstanden

Ich bin damit einverstanden, dass der Titel meiner Arbeit mit meinem Namen und denen der Betreuer im Bibliothekskatalog (OPAC) veröffentlicht wird und die Arbeit als PDF hochschulintern eingesehen werden kann. Dafür erhält die Hochschule ein einfaches, nicht übertragbares Nutzungsrecht ausschließlich für den Zweck der Veröffentlichung in der Bibliothek. Das Recht der Veröffentlichung oder Verwertung durch den Verfasser oder die Verfasserin auf andere Weise, z.B. über einen Verlag, bleibt davon unberührt. Die Hochschule ist nicht verpflichtet, die Arbeit zu veröffentlichen. Das Einverständnis kann jederzeit schriftlich (per Brief!) widerrufen werden. Die Bibliothek wird die Arbeit dann unverzüglich aus dem OPAC oder der Auslage entfernen. Die Veröffentlichung hängt außerdem von der später erteilten Zustimmung des Erstbetreuers ab.

München, 25.05.2016

---

Unterschrift

## Sperrvermerk

Der vorliegende Praxisprojektbericht enthält vertrauliche Daten und Informationen der Simi Reality Motion Systems GmbH, die nicht für die Öffentlichkeit bestimmt sind. Der Inhalt der Arbeit, auch auszugsweise, darf nur mit Genehmigung der Simi Reality Motion Systems GmbH an Dritte außerhalb der Hochschule Koblenz weitergegeben werden.

The analysis of human motion is a highly relevant topic in many fields of application. The conventional method of motion analysis is based on retro reflective markers which are attached to the body to mark important points. Markerless tracking is seen as a potential method to make motion analysis simpler and quicker. The aim of this study was to evaluate the accuracy of markerless tracking against marker based tracking with reducing cameras to make the application cheaper. For this, various movements were tracked with eight, six, four and three cameras and then compared with each other in order to test the influence of fewer cameras on the data accuracy. Joint angles of hip, knee, elbow, shoulder and ankle of markerless tracking are compared to joint angles of marker tracking by means of correlation coefficient and standard deviation of angle difference. The correlation coefficient is always relating to marker based data. It should be noted that the effort of tracking may rise with fewer cameras, because the model needs to be readjusted more often. Problems of markerless tracking especially occur for joint rotations for which the silhouettes of the body segments barely change. Furthermore the center of mass and the velocity and acceleration of segment center of mass are also compared with the aid of correlation coefficient. These data are more important for sports questions. Good results can be achieved in this area for all setups even for tracking with three cameras. Markerless tracking with less than eight cameras is possible. To keep the effort of tracking as low as possible, working with at least four cameras is recommended. The tracking process is fast and can be achieved without major adjustments to the model. Based on these results, the effect on the accuracy of kinematic data will be investigated in the second part of this work when tracking with cameras with an inferior quality. Especially in the field of sports, large camera systems are very complex and require a lot of time to install them. Small and mobile systems would be better to do quick analysis on a sports field and are very cost efficient. Long cables and complicated constructions would be no longer necessary. Therefore the difference between GoPro<sup>®</sup> cameras and normal high speed cameras was examined in this study. GoPro<sup>®</sup> cameras allow recordings without a PC in the outdoor. This study discusses the body center of mass, segment velocity and segment acceleration, which are very important in sports. Tracking with four GoPro<sup>®</sup> cameras are going well, problems arise due to the velocity of the movement. Nevertheless some good correlations can be achieved. The center of mass calculated by the GoPro<sup>®</sup> data does not differ from the markerless high speed data. Also in the joint centers and the segment velocity good correlations can be achieved. GoPro<sup>®</sup> cameras are suitable for marker less tracking if the velocity of the movement is not too high.

# Contents

<b>I</b>	<b>Introduction and Motivation</b>	<b>1</b>
<b>II</b>	<b>Effects on marker less 3D joint position and angle accuracy using eight vs. six, four and three high speed cameras</b>	<b>3</b>
<b>1</b>	<b>Theoretical background</b>	<b>4</b>
1.1	Technical equipment, system setup and calibration . . . . .	4
1.2	Methods of motion tracking . . . . .	5
1.3	Software used . . . . .	6
1.3.1	Simi Motion 3D . . . . .	6
1.3.2	Simi Shape . . . . .	8
1.4	Basic anatomy . . . . .	9
1.4.1	Body planes and axes . . . . .	9
1.4.2	The human joint and its possibilities of movements . . . . .	10
<b>2</b>	<b>Methods</b>	<b>12</b>
2.1	Description of camera setups used . . . . .	12
2.1.1	Jumping-Jack . . . . .	12
2.1.2	Biking . . . . .	13
2.1.3	Running . . . . .	14
2.1.4	Jump . . . . .	15
2.1.5	Kick and box . . . . .	15
2.1.6	General procedure . . . . .	16
2.2	Tracking settings and statistical comparison . . . . .	16
2.2.1	Filtering data . . . . .	17
2.2.2	Statistical comparison . . . . .	17
<b>3</b>	<b>Results</b>	<b>21</b>
3.1	Influence of model initialization to tracking results . . . . .	21
3.2	Results of joint angles . . . . .	22
3.2.1	Jump: both legged . . . . .	22
3.2.2	Jump: right leg only . . . . .	23
3.2.3	Jumping-Jack . . . . .	25

---

3.3	Results of 3D joint position accuracy . . . . .	26
3.3.1	Average of segment velocity and acceleration over all movements . . . . .	26
3.3.2	Segment center of mass of the movement Jump . . . . .	27
3.3.3	Segment velocity and acceleration of the movement Jump . . . . .	28
<b>4</b>	<b>Summary</b>	<b>31</b>
<b>III</b>	<b>Effects on markerless 3D joint position accuracy using GoPro<sup>®</sup> cameras</b>	<b>33</b>
<b>5</b>	<b>Expanded Basics</b>	<b>34</b>
5.1	Technical Equipment . . . . .	34
5.2	Image processing . . . . .	36
5.2.1	Theoretical bases of optics . . . . .	36
5.2.2	GoPro <sup>®</sup> cameras . . . . .	36
5.2.3	Basler Scout scA640-120gm . . . . .	40
<b>6</b>	<b>Expanded Methods</b>	<b>43</b>
6.1	Data capture setup using high speed and GoPro <sup>®</sup> cameras . . . . .	43
6.2	Special problems when tracking with GoPro <sup>®</sup> cameras . . . . .	45
<b>7</b>	<b>Results</b>	<b>47</b>
7.1	Volleyball . . . . .	47
7.1.1	Position of joint centers . . . . .	47
7.1.2	Body center of mass (COM) . . . . .	49
7.1.3	Segment velocity and acceleration . . . . .	50
7.2	Handball . . . . .	51
7.2.1	Joint center . . . . .	51
7.2.2	Body center of mass (COM) . . . . .	51
7.2.3	Segment velocity and acceleration . . . . .	52
7.3	Basketball . . . . .	53
7.3.1	Joint center . . . . .	53
7.3.2	Body center of mass (COM) . . . . .	54
7.3.3	Segment velocity and acceleration . . . . .	55
7.4	Total Result . . . . .	56
7.4.1	Joint center . . . . .	56
7.4.2	Body center of mass (COM) . . . . .	57
7.4.3	Segment velocity and acceleration . . . . .	58

---

<b>8 Summary</b>	<b>59</b>
<b>IV Discussion of the evaluation of markerless 3D joint position accuracy using high end vs. low end camera setups</b>	<b>62</b>
<b>Bibliography</b>	<b>64</b>
<b>A Appendix</b>	<b>66</b>

# List of Figures

1.1	Camera with lenses and ring lights [7, p.50]	4
1.2	L-Frame and T-Wand [7, p.123]	5
1.3	Markerpositions of the full body marker set	7
1.4	Jump in the curve of Manubrium sterni	7
1.5	3D stick view in comparison	8
1.6	Initialization pose	9
1.7	Body planes based on [19]	10
1.8	Joint types with examples based on [18]	11
1.9	Possible movements [12]	11
2.1	Camera Setup: Jumping-Jack	13
2.2	Comparison between original and edited recording	14
2.3	Camera setup: Biking	14
2.4	Camera setup: Running, jumping and kick boxing	15
2.5	Shape model	17
2.6	Effect of different cut-off frequencies	18
2.7	Calculation of Spearman's correlation coefficient in Libre Office calc	19
3.1	Jump: initialization pose	22
3.2	Both legged jump: right elbow	23
3.3	Both legged jump: pelvis problems	23
3.4	Right legged jump: shoulder and 3D figure	24
3.5	Jumping-Jack: Tilt pelvis and the effect on the data	25
3.6	Jumping-Jack: 3D figure thigh	26
3.7	Diagram: Average over all movements for each segment	27
3.10	Jump: Body focus	29
3.11	Jump: Comparing joint centers	30
3.12	Both legged jump: Velocity and acceleration of segment	30
5.1	Distortation correction	34
5.2	calibration system	35
5.3	Optical path	36
5.4	GoPro <sup>®</sup> camera: blurred	37
5.5	GoPro <sup>®</sup> camera: 240fps	39
5.6	GoPro <sup>®</sup> camera: 120fps	39
5.7	GoPro <sup>®</sup> camera: 60fps	40
5.8	Influence of different shutter speeds	40

---

6.1	Comparison of speeds between two different throws . . . . .	44
6.2	Camera setup gym . . . . .	44
6.3	Test: Effect on the accuracy of the setting <i>ipf</i> . . . . .	45
7.1	Volleyball: Comparing joint centers . . . . .	48
7.2	Volleyball: COM . . . . .	49
7.3	Volleyball: segment velocity and acceleration . . . . .	50
7.4	Handball: Joint centers . . . . .	51
7.5	Handball: COM . . . . .	52
7.6	Handball: segment velocity and acceleration . . . . .	53
7.7	Basketball: Comparing joint centers . . . . .	54
7.8	Basketball: body center of mass . . . . .	55
7.9	Basketball: Model overlay . . . . .	55
7.10	Basketball: segment velocity and acceleration . . . . .	56
7.11	Total result: Joint centers . . . . .	57
7.12	Total result: COM . . . . .	58
7.13	Total result: segment velocity and acceleration . . . . .	58
8.1	Discussion: Filtering . . . . .	60
8.2	Discussion: Comparison between 120Hz and 60Hz . . . . .	61
A.1	Velocity+Acceleration of segment focus Jumping: Right leg only . . . . .	77
A.2	Velocity+Acceleration of segment focus Jumping: Left leg only . . . . .	77
A.3	Velocity+Acceleration of segment focus Jumping: both legs . . . . .	77
A.4	Velocity+Acceleration of segment focus Running: large steps . . . . .	78
A.5	Velocity+Acceleration of segment focus Running: small steps . . . . .	78
A.6	Velocity+Acceleration of segment focus Kickbox . . . . .	78



# List of Tables

2.1	Cohen's classification . . . . .	19
2.2	Classification of correlation coefficient . . . . .	19
3.1	Both legged jump: Hip . . . . .	23
3.2	Right legged jump: Shoulder . . . . .	24
3.3	Both legged jump: upper leg . . . . .	29
5.1	Example parameter GoPro <sup>®</sup> Hero 3 White edition . . . . .	38
5.2	Example parameter GoPro <sup>®</sup> Hero 4 Silver edition: 240fps . . . . .	38
5.3	Example parameter GoPro <sup>®</sup> Hero 4 Silver edition: 120fps . . . . .	39
5.4	Example parameter GoPro <sup>®</sup> Hero 4 Silver edition: 60fps . . . . .	39
5.5	Example parameter High speed camera: $t_s = 2$ ms . . . . .	41
5.6	Example parameter High speed camera: $t_s = 8$ ms . . . . .	41
5.7	Example parameter High speed camera: $t_s = 10$ ms . . . . .	42
7.1	Volleyball: Knee . . . . .	48
7.2	Volleyball: COM . . . . .	49
7.3	Handball: COM . . . . .	52
7.4	Basketball: Knee . . . . .	53
A.1	Velocity and acceleration . . . . .	66
A.2	Velocity and acceleration . . . . .	66
A.3	Position of Joint centers . . . . .	67
A.4	Jump: Both legs . . . . .	68
A.5	Jump: Right leg . . . . .	69
A.6	Jump: Left leg . . . . .	70
A.7	Kick and Box . . . . .	71
A.8	Biking . . . . .	72
A.9	Jumping Jack . . . . .	73
A.10	Running: Small steps . . . . .	74
A.11	Running: Large steps . . . . .	75
A.12	Average over all movements and right/left . . . . .	76
A.13	Joint centers of Volleyball . . . . .	79
A.14	Joint centers of Handball . . . . .	79
A.15	Joint centers of Basketball . . . . .	80
A.16	Joint centers: Average over all movements . . . . .	80
A.17	Segment velocity and acceleration of Volleyball . . . . .	81
A.18	Segment velocity and acceleration of Handball . . . . .	82

A.19 Segment velocity and acceleration of Basketball . . . . .	83
A.20 Average over all movements of segment velocity and acceleration . . .	84

## List of abbreviations

<b>COM</b>	Center of mass
$d$	distance
$\varepsilon$	pixel size
$f$	focal distance
<b>fps</b>	frames per second
$f_r$	frame rate
<b>ipf</b>	iterations per frame
$m_L$	lateral projection level
<b>px</b>	pixel
$q$	resolution of the video
$r_s$	Spearman's correlation coefficient
$\sigma$	standard deviation
$t_s$	shutter speed
$x$	object size
$x'$	displayed object size
$X_c$	resolution of the chip

# **Part I**

## **Introduction and Motivation**

# Introduction

## Simi Reality Motion Systems GmbH

Simi Reality Motion Systems GmbH (Simi), was founded in 1992 by Andreas Russ. The company specializes in the development, production and distribution of products in the field of exercise and behavioral analysis. Simi is an international company with distributors around the world. A few years ago the subsidiary company Simi US Motion was founded. Simi systems are camera-based and use industrial cameras in combination with a workstation. There are three different products when it comes to motion analysis. They mainly differ in complexity, operational effort and data quality. The first product is MotionTwin for easy and fast records. The second one is Simi Aktisys, which focuses on fast acquisitions and results, using only one or two cameras. The last one is Simi Motion 3D, it enables the user to create accurate 3D calculations based on the positions of reflecting markers attached to the subjects. There are some additional systems. For example Simi BioCell, for cell growth observation. Another software is Simi Scout, which enables tactic analysis of team sports to illustrate courses.

## Motivation

The analysis of human motions is a highly relevant topic in many fields of application. The visualization of movements in sports is an important approach to spot technical deficits and potentials for movement optimization to improve individual sports performances. Also in medical field, motion analysis is very important e.g for prosthetic fitting. A movement is recorded by cameras. Usually retro reflective markers are used to capture the kinematic data. These markers are attached to the body on certain points and denote joint centers. This harbors a high potential for errors. With the marker positions 3D coordinates can be calculated and joint angles are determined. The software Simi Motion 3D is able to track the markers. The new software Simi Shape is able to track movements without markers, using silhouettes instead. For an analysis with Simi Shape eight cameras are used which is the only setup that has been evaluated to date [2]. An analysis outside the laboratory is difficult to realize because each camera must be connected with two cables which can be an issue when using a usual computer, unless wireless cameras such as action cameras will be used. The aim of this study is to capture kinematic data using less than eight cameras to offer coaches and sport science institutes a system with a high accuracy of data but less cost of effort. More testing will be done in this study if the results, of tracking with less than eight cameras, are good. GoPro<sup>®</sup> cameras are used, because the flexibility of the system increased by using action cameras.

## **Part II**

**Effects on marker less 3D joint position and angle accuracy using eight vs. six, four and three high speed cameras**

# 1 Theoretical background

This chapter will firstly present the technical system, used to record movements. Next the different possibilities of motion tracking will be explained. Finally there will be a short overview of the analyzed joints.

## 1.1 Technical equipment, system setup and calibration

All recordings were made in the Simi laboratory. The laboratory is equipped with eight Basler scA640 - 120cg cameras, which acquire videos with a frame rate of up to 120 Hz and a resolution of 658x492 pixels. Mounted to the cameras are Fujinon 3.8-13mm DV3.4x3.8SA-1 lenses. All eight cameras are synchronized by a dedicated IO box, which sends out a square wave signal for every frame that should be obtained. The IO box is connected to the cameras with trigger cables. Those cables do not only trigger the cameras, but also provide power supply. Network cables allow broadcasting the videos live in Simi Motion to control the acquisition.



**Figure 1.1:** Camera with lenses and ring lights [7, p.50]

As seen in Figure 1.1 additional ring lights with 72 LEDs are mounted on all cameras. The ring lights are powered through the same trigger cables as the camera. Another substantial part of the system are retro reflective markers, which are used on the calibration devices and on the tested subject. The light provided by the ring lights is reflected by the markers and enables better marker recognition by the software. In the videos the markers appear as white spots and can be tracked by the software. The first step before recording is the calibration. This is done with a calibration wand of exactly known size and a L-Frame for setting the 3D coordinate system [7, pp. 122] (according to Figure 1.2). The wand has to be moved through the room to be captured with all cameras in different perspectives. After

acquisition, the videos are automatically tracked and the markers automatically assigned. Finally the calibration is computed and validated. A good calibration should have a standard deviation of  $\leq 1mm$ . The distance of the marker has an accuracy of  $\leq 1mm$ .



Figure 1.2: L-Frame and T-Wand [7, p.123]

## 1.2 Methods of motion tracking

There are two possibilities to analyze movements. They differ in the type of the cameras. The first possibility is an image-based technique. Synchronized industrial cameras record the motion and by means of image processing algorithms the markers are tracked and 3D coordinates can be calculated. Simi Reality Motion Systems GmbH uses this method. The second possibility is to use infrared cameras. Retro reflective markers reflect infrared light to cameras and thereby 3D coordinates of markers are calculated. Vicon is a leading company in this field. For both systems retro reflective markers are needed to calculate kinematic data. The new technology of Simi is the silhouette-based tracking. This technology is able to track human motions markerless or as a hybrid variant, which means that some markers support the silhouette-based tracking.

## 1.3 Software used

In this study two products of Simi were used. On the one hand Simi Motion 3D (Version 2.2.0) and on the other hand Simi Shape 3D (Version 2.2.0). Simi Shape is an extension of Simi Motion. With this software the markerless and the hybrid data can be calculated. The software is explained below.

### 1.3.1 Simi Motion 3D

Simi Motion 3D is an image-based system as explained before. Retro reflective markers are placed at specific points on the body. The software is able to detect the markers and to calculate 3D data from it. This requires that all markers are recognized in every frame from at least two cameras. The human body consists of 16 segments (foot, upper/lower leg, upper/lower arm, head, wrist, upper/lower torso and pelvis) that are linked by joints. The markers determine both the position of the joint and the center of gravity (COG) of each segment. Furthermore the local coordinate systems are defined by the markers. The origin is located at the COG of the segment. The joint centers of ankle, knee, elbow and wrist are defined as the center of the connection line between the medial and lateral markers of the particular joint [7, p. 365f]. Hip and shoulder joints are calculated in a more complex way according to the works of Bell et al.[3] and De Leva[15]. In addition to the local segment coordinate system, there are joint coordinate systems, which are based on the International Society of Biomechanics (ISB). With the aid of the joint coordinate systems the joint angles are calculated. Each segment consists of two coordinate systems, one of the distal and one of the proximal segment. Joint angles are described as rotations between the two joint coordinate systems. They are given as a rotation matrices and are then converted to xyz-Cardan angles. The first angle describes a rotation around the x-axis. The rotation of the distal segment is outputted as the rotation of the proximal coordinate system[7, pp. 370 & p. 374].

In this study the full body marker set (according to Figure 1.3) was used. At the beginning of each experiment a static trial has been recorded. Therefore additional markers are needed, which are removed for the dynamic recording to prevent marker jumps. These markers are shown in blue in Figure 1.3. The subject is standing in an upright position with the arms hanging straight besides the body. This pose is used for calculating person-specific data such as the lengths of body segments and the location of joint axes. Following the initializing pose the dynamic recording can be started. After the dynamic trial each marker must be assigned manually in one frame for at least two cameras to get 3D coordinates. This frame is the initialization frame and the assignment for the rest recording is done automatically using this frame. During this process errors may occur. The markers can jump from



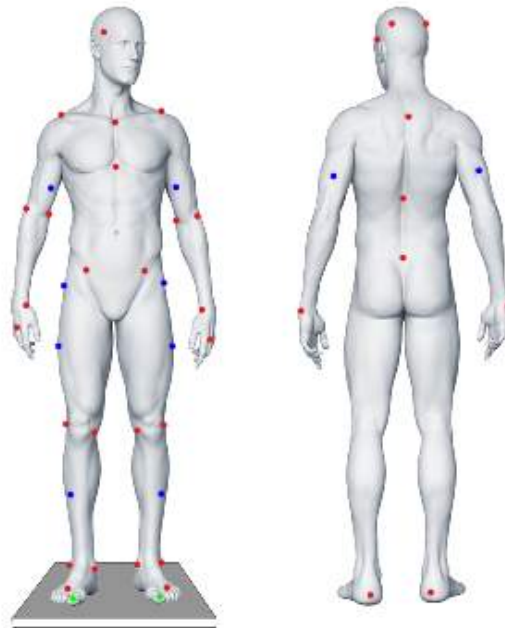


**Figure 1.3:** Markerpositions of the full body marker set

one point to another. This error can be clearly seen in the curve of the markers. If a marker was assigned incorrectly it is visible as a jump in the curve as shown in Figure 1.4. This can be corrected manually. Another possible mistake is, that one marker is not assigned in at least two cameras. Therefore 3D coordinates can not be calculated. Missing markers are best seen in 3D stick view. Then lack the 3D-coordinates of a marker the connecting line between two markers is not shown. Figure 1.5 shows an erroneous 3D stick view in comparison to a correct one. Before the inverse kinematics can be calculated, all errors must be corrected.

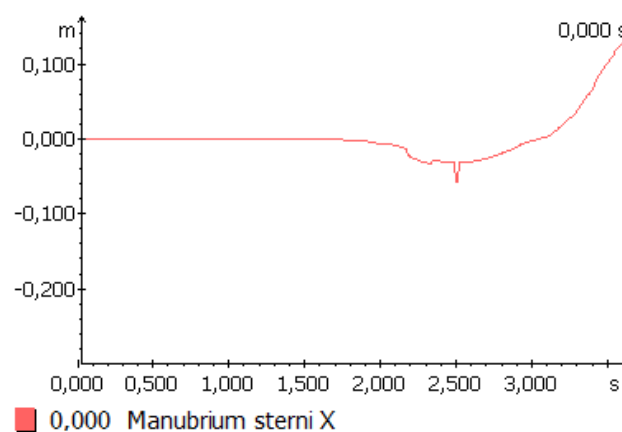


**Figure 1.4:** Jump in the curve of Manubrium sterni

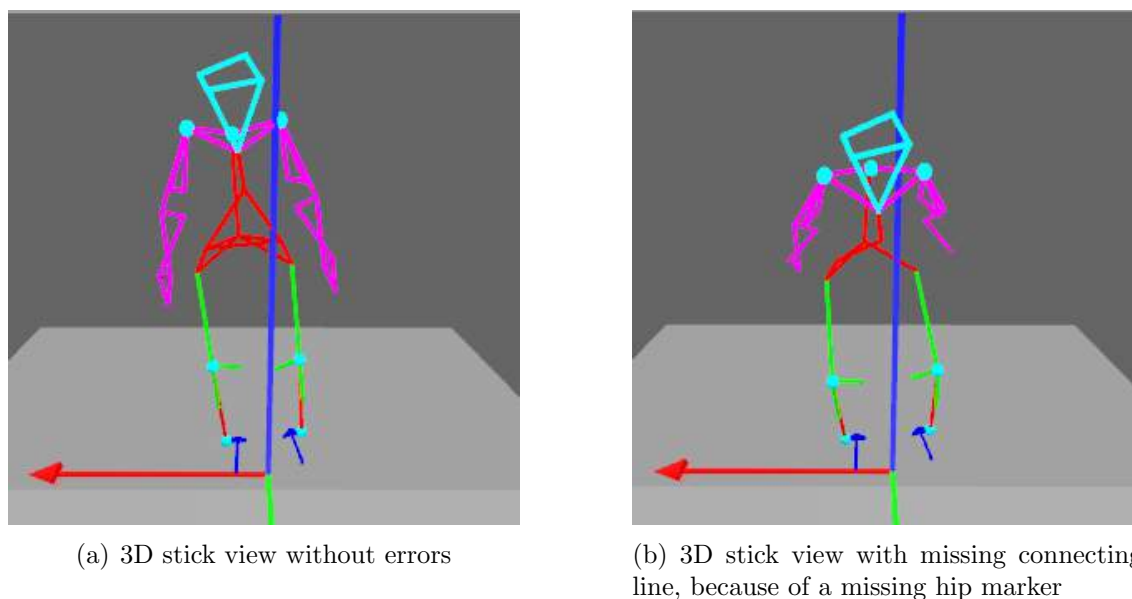


**Figure 1.5:** 3D stick view in comparison

### 1.3.2 Simi Shape

Simi Shape is integrated in Simi Motion. All possibilities of data processing and data acquisition are still done by Simi Motion. Only the tracking process takes place in Simi Shape. Simi Shape allows to track movements without any markers. It is based on the silhouette to which a mathematical model is adjusted. The camera setup and calibration procedure is the same as for marker based tracking in Simi Motion. Ringlights are not needed for the dynamic recording as no reflective markers have to be lighted. To achieve a good tracking result the following aspects should be considered. It is important to have a good contrast between the subject and the background [8, p. 29]. To ensure this all trials in this study were performed with a tight fitting, colored morphsuit. Another important point is, that the subject should be clearly visible and as large as possible in all cameras. The process of markerless tracking can be divided into three steps: segmentation, model initialization and tracking. The first step is the background subtraction. Two recordings are needed that are taken under the same conditions [8, p. 13]: one with the subject, and one without the subject. The software compares the color and intensity of each pixel in each camera during the background subtraction. If the difference compared with the upper threshold in at least one color channel is too high, the pixel is assigned to the subject. There is also a lower threshold. If the difference in all color channels is less than this lower threshold value, the pixel is assigned to the background [8, p. 56]. In the next step, model initialization, a mathematical 3D model is fitted into the silhouette. At the beginning of each movement an initialization pose, called psi-pose, is performed by the subject. In this pose the subject is slightly bent with bent

arms. In Figure 1.6 the psi pose is shown. The joint positions can be determined. The mathematical model can automatically adjust itself to the silhouette, both in position and in the length and thickness of the segments. Once the model is well adjusted, the tracking process can be started. For this purpose the iterative closest point (ICP) algorithm is used. The algorithm is looking for similarities between the silhouette and the model and is able to fit the current pose of the model to the current pose of the silhouette [8, p. 69]. During the tracking process it may happen that the model loses the silhouette. In that case the tracking process can be interrupted and the model readjusted. The joint angles can be exported to Simi Motion.

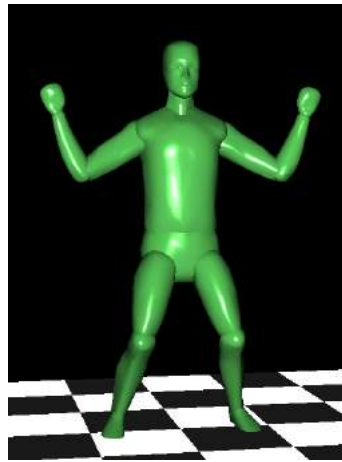


Figure 1.6: Initialization pose

## 1.4 Basic anatomy

### 1.4.1 Body planes and axes

The body can be divided in three main axes. These are used in anatomy to be able to describe certain structures or directions. The three main axes are the following:

**Longitudinal axis** It runs from top to bottom and corresponds to the mathematical y-axis

**Sagittal axis** It runs from front to back and corresponds to the mathematical z-axis

**Transverse axis** It runs from right to left and corresponds to the mathematical x-axis

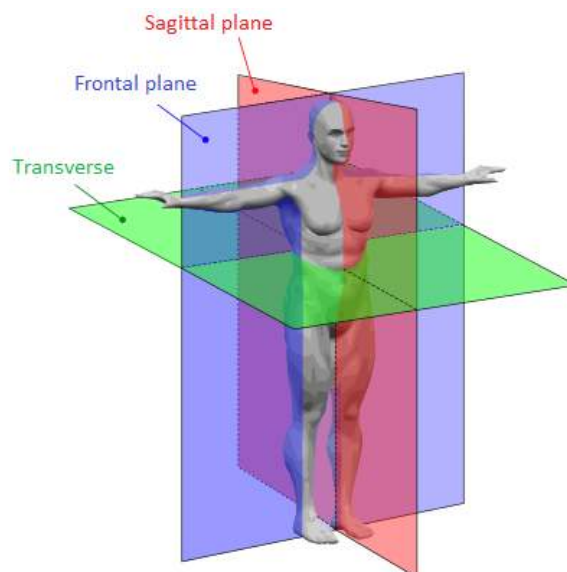


**Figure 1.7:** Body planes based on [19]

According to the axes body planes are defined as:

**Frontal plane** Defined by the longitudinal axis and the transverse. In Figure 1.7 shown as the blue colored plane.

**Sagittal plane** Defined by the longitudinal axis and the sagittal and divides the body into two symmetrical halves. The red colored plane in Figure 1.7

**Transverse** Defined by the transverse axis and the sagittal and divides the body into an upper and lower half. Shown as the green colored plane in Figure 1.7

### 1.4.2 The human joint and its possibilities of movements

A joint is a flexible connection between two or more bones. To enable movements, muscles are connected to the bones by tendons. The human joints can be divided into two groups. There are the real joints, called Diarthrose and the false joints called Synarthrose. Only real joints have a joint space. It separates joint surfaces which are covered with joint cartilage. Furthermore, the joint is surrounded from the outside with a tight joint capsule. There are five different joint types, which differ in the joint surface. The first joint, is the ball joint, which can move in all directions and thus has three degrees of freedom. Secondly, there is the condyloid joint. It can perform bending and stretching movements and side-to-side movements. The saddle joint is only biaxial with two degrees of freedom. And the last type of joints is the cylinder joints. Cylinder joints include the hinge and pivot joints and are uniaxial joints that only have one degree of freedom and thus allow only movements around one axis. All declared joints are presented in Figure 1.8.

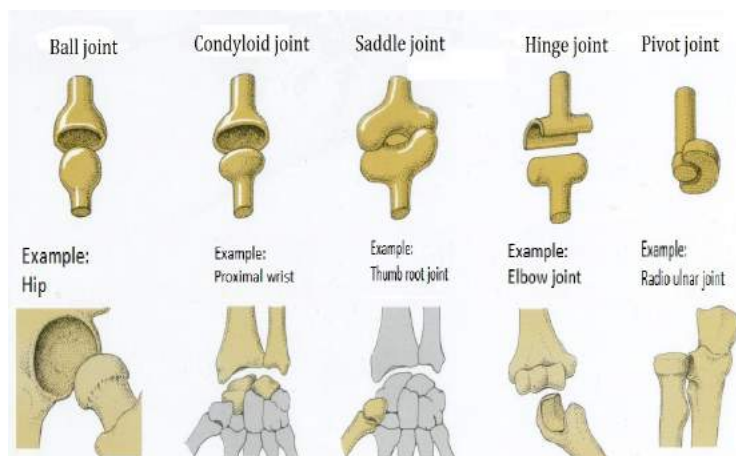


**Figure 1.8:** Joint types with examples based on [18]

Movements in the frontal plane around the sagittal axis are called Ab-/Adduction. Bending and stretching of a body part are called Flexion or Extension. And the third movement in the transverse is called internal and external rotation [13]. Figure 1.9 visualizes the possible movements.

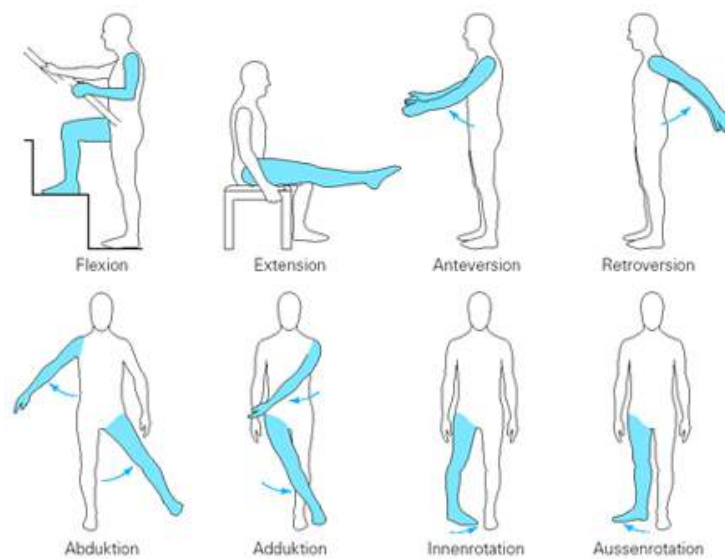


**Figure 1.9:** Possible movements [12]

## 2 Methods

This chapter will present the methodical approach of this work. It will describe the tracking process and the statistical analysis, which is needed to compare the results with each other.

### 2.1 Description of camera setups used

In this work the influence of fewer cameras on the accuracy of the kinematic data will be examined because until now only setups with eight cameras were tested. Several movements were recorded using eight cameras. For the analysis cameras were deleted from the recordings in order to use less information from a few cameras for silhouette based tracking. For the comparison value marker based data of eight cameras were used. Eight cameras are necessary to ensure that sufficient information exists to calculate 3D data. It should be noted that, the camera setup is built for eight cameras. In some cases, the remaining cameras should be positioned differently. The following section describes which camera was deleted in which setup. There are five different movements: Biking, Running, Jumping, Jumping-Jack and Kick boxing. At first, six cameras were used, then four and finally three.

#### 2.1.1 Jumping-Jack

The subject was standing on the floor with their view into the room. Extra care has been taken to avoid changing light conditions that could have influenced the image quality otherwise the background segmentation does not work well, as described in subsection 1.3.2. The camera setup is shown in Figure 2.1. The cameras 1, 3, 4, and 7 filmed from above. The others filmed from hip height. For good tracking results it is important to see the subject as large as possible. Camera 4 was filming the movement from a greater distance. This led to a loss of information because the subject was too small. Camera 6 filmed from the sagittal plane. The problem was that the movement of the right arm was not visible. Because of that, both cameras were removed. The position of the cameras 1 and 2 were very similar. Recordings from the frontal plane are more meaningful because the abduction and adduction of hip and shoulder can be better filmed. So camera 1 was removed. Camera 3 has a similar problem as camera 6. The left arm was obscured very often by the body. Finally, camera 7 was removed.

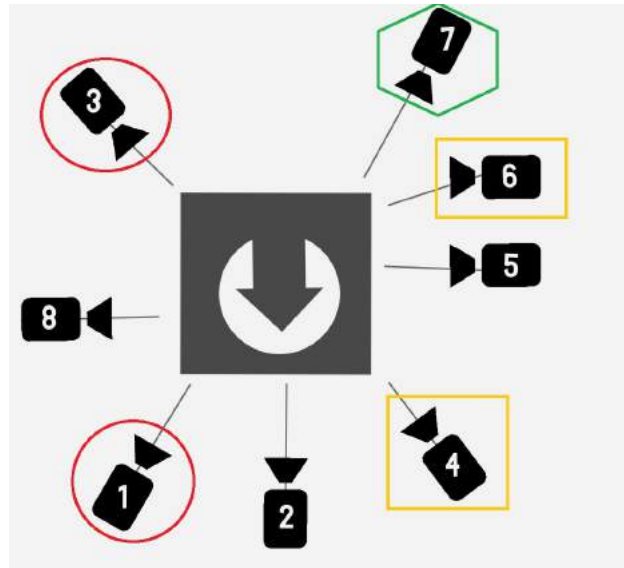


**Figure 2.1:** Camera Setup during Jumping-Jack (deleted cameras are marked)  
 yellow rectangle: 6 cameras, red circle: 4 cameras, green hexagon: 3 cameras

### 2.1.2 Biking

This movement was executed on a road bike with a bicycle trainer. The light conditions were really bad in this recording. There was no good contrast so that the background subtraction did not work. The brightness can be adjusted through image processing. The difference is clearly visible in Figure 2.2. In the right image the brightness was increased by 70%. Figure 2.3 shows the camera setup for this experimental setup. In this case there was no recognizable abduction/adduction. Filming from the frontal plane was useless. For this reason camera 4 was removed. For the software it is very hard to differentiate between arm and leg when one is above the other. In camera 2 a differentiation was not possible. Camera 3 was another frontal camera which was deleted for the above reasons. In camera 5 the right arm was not visible. In the end camera 8 was removed, the left arm was also not visible.

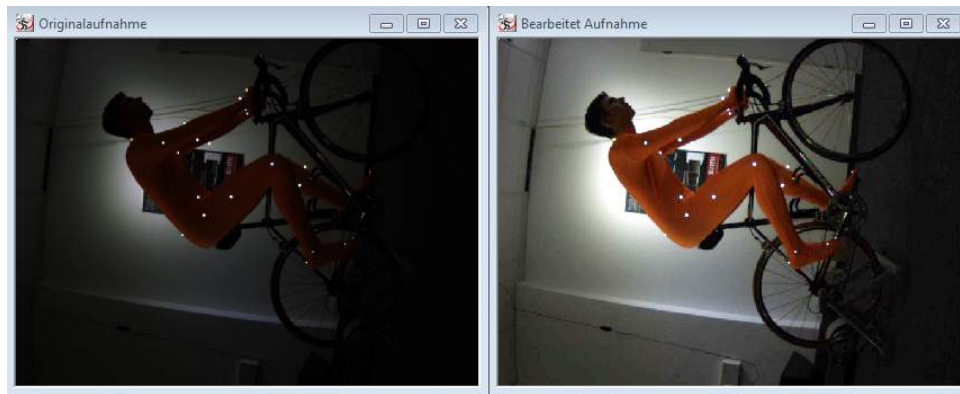


**Figure 2.2:** Comparison between original and edited recording

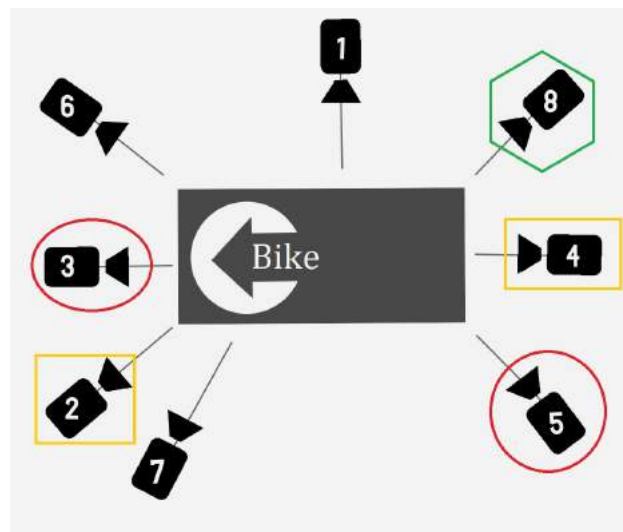


**Figure 2.3:** Camera setup during biking (deleted cameras are marked)  
 yellow rectangle: 6 cameras, red circle: 4 cameras, green hexagon: 3 cameras

### 2.1.3 Running

This movement was carried out on a treadmill. The camera setup is shown in Figure 2.4. During this recording the subject was running with different step lengths. First with big steps and then with small steps. The analysis will decide between the different step lengths. Camera 2 and 7 were very similar on the settings. Due to that one of two was removed. Camera 2 was filming from above which was the main advantage against camera 7. There were two frontal cameras which return almost the same results. Because of that camera 4 was deleted. Now there were four cameras in each corner, one in the sagittal and one in the front. The frontal and sagittal camera were very important and provide essential information. If two diagonally positioned cameras were removed there is a small loss of information. So one camera filmed from ahead, and one from the back. The camera setting of camera 2 was very good and should be retained. Therefore camera 8 can not be



deleted. Thus camera 5 and 6 were deleted. As explained before, camera 1, 2 and 3 were indispensable and thus the remaining cameras.

### 2.1.4 Jump

This movement was carried out on the treadmill as well. The camera setup was the same as in the previous experiment (according to Figure 2.4). Three different types of jumps were performed. First jumping with both legs, then with the right leg only and finally with the left leg only. The analysis decides between the different types. The cameras 7 and 4 were removed for the same reasons mentioned above. In contrast to the previous case, camera 6 and 7 were deleted. The left body side was captured from camera 1 sufficiently. In the end camera 5 was removed.

### 2.1.5 Kick and box

The conditions (location of execution and camera setup) were the same as in the previous two experiments. Camera 7 was removed for the same reasons mentioned above. Unlike in the previous trial camera 3 was deleted. A chair concealed the view onto the half of the leg. Camera 6 and 8 were dislodged for the same reasons as in the experiment *Jump*. Other than in experiment *Jump* camera 2 was removed in the end.

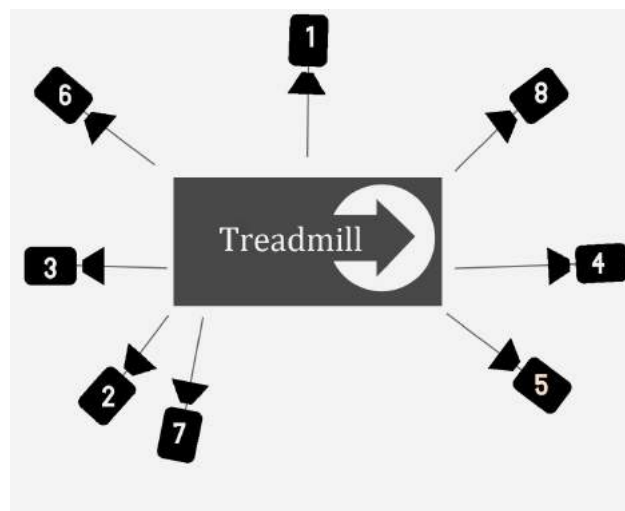


**Figure 2.4:** Camera setup during running, jumping and kick boxing

### 2.1.6 General procedure

If only four cameras are used, some aspects have to be considered in general to get enough information for a good tracking process. The subject should be seen as large as possible. This is necessary to differentiate, for example, between both legs. Furthermore one camera from the sagittal plane and one from the frontal plane is required in order to get information about ab-/adduction and flexion/extension. It should be ensured that at least one camera is filming from above. The last camera should film the other side of the body.

## 2.2 Tracking settings and statistical comparison

All experiments were recorded in the laboratory of Simi Reality Motion Systems. The five described movements were carried out by three different male subjects. Eight high speed cameras with a frame rate of 100Hz were used. All subjects wore a tight colored morphsuit with the markerset described in subsection 1.3.1 attached. Thus the same recording can be used for the marker based and markerless evaluation. The tight colored morphsuit is not necessary but was used to ensure a good segmentation as described in subsection 1.3.2.

Markerless data obtained from setups with six, four and three cameras were compared to marker based data from eight cameras. On the one hand joint angles were evaluated by means of correlation coefficient and the standard deviation of angles difference were compared. On the other hand the velocity and acceleration of segment center of mass (COM) were calculated and compared using the correlation coefficient. The COM was calculated automatically through a prefabricated template which divides the body into its elements to get the segment COM. Another template calculated the velocity and acceleration automatically and emitted them for each segment. The body is divided into 14 segments. In the analysis wrist and feet are disregarded due to the small mass. The analysis deals only with upper/lower arms, upper/lower legs, head and torso. Furthermore the whole COM was considered. This data is very important for sports. Splitted movements in the three axes are insignificant.

In this study only the following five joints were tested in the indicated directions.

**Hip** Flexion/Extension, Ab-/Adduction, internal/external rotation

**Knee** Flexion/Extension

**Ankle** Plantar/Dorsal Flexion, Eversion/Inversion, Ab-/Adduction

**Shoulder** Flexion/Extension, Ab-/Adduction, Internal/External rotation

## Elbow Flexion/Extension

In contrast to the real joints the knee and elbow joint have only one degree of freedom in the Shape model. Thus only movements of flexion and extension are shown. The hand is displayed as a ball in the model and does not change its silhouette as shown in Figure 2.5. Because of that the wrist is neglected in the analysis. For the same reason the head is hard to track and is also not considered.

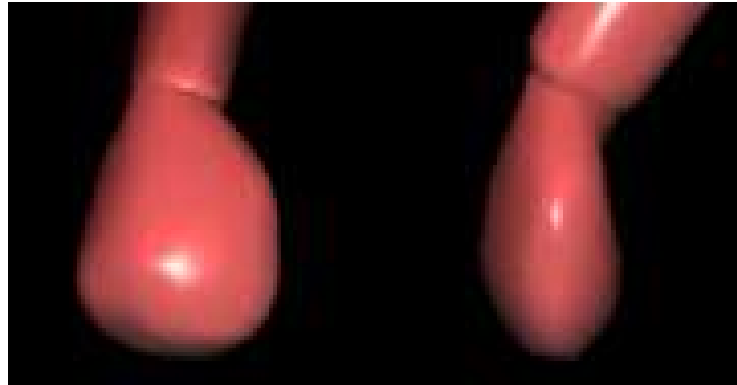


**Figure 2.5:** Hand of the model from two different perspectives

### 2.2.1 Filtering data

All data obtained by Simi Motion and Simi Shape are filtered with a 6Hz 2nd order low pass. These values are orientated on Richards for walking. For faster movements he recommends using higher cut-off frequencies [16, p. 114]. Dal. Pupo et al [4] as well as Willson et al. [20] use a cut-off frequency of 10Hz for analyzing jumping movements. Therefore the effect of different cut-off frequencies was tested at the experiment *jump*. Figure 2.6 shows the curve of the right ankle during the both legged jump. The red curve was filtered with 6Hz and the blue one with 10Hz. A slight difference can be seen. Comparing data with the aid of correlation coefficient brings a match of  $r_s \sim 0,99$ . The different filter frequency has no major effect on the results. A filter frequency of 6Hz was chosen to ensure a standardized evaluation.

### 2.2.2 Statistical comparison

In order to make a statement about the accuracy of two data sets, the data must be evaluated by the means of correlation coefficient. The most common correlation coefficient is the Pearson correlation coefficient (1865). This can only be applied if the data is normally distributed. This is not the case in the present data. The concept of Pearson does not apply. Spearman's rank correlation coefficient is a non parametric measure for correlations and can be applied in this case [17, p. 102].

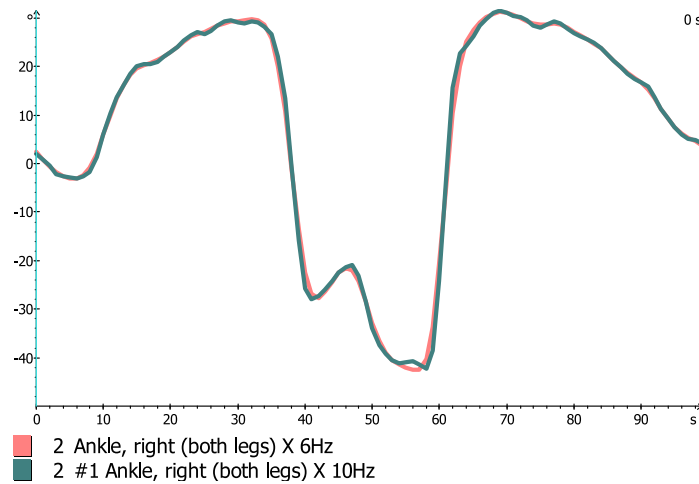


**Figure 2.6:** Effect of different cut-off frequencies on the results  
red: 6Hz, blue: 10Hz

The symbol is  $r$ , especially for Spearman's correlation coefficient the symbol is  $r_s$ . Correlations take on a value of -1 to +1. If a value is close to  $r = +1$  a high correlation is available. For values close to  $r_s = -1$  a negative correlation exists. This means that the curves are very similar but symmetrical to the x-axis. For the case  $r = 0$ , the data do not correlate with each other [17, S. 98ff]. The formula reads as follows:

$$r_s = \frac{\sum_{i=1}^n x_i y_i - (\sum_{i=1}^n x_i \cdot \sum_{i=1}^n y_i)/n}{\sqrt{\sum_{i=1}^n x_i^2 - (\sum_{i=1}^n x_i)^2/n} \cdot \sqrt{\sum_{i=1}^n y_i^2 - (\sum_{i=1}^n y_i)^2/n}} \quad (2.1)$$

The sum of the ranks is always  $\frac{n(n+1)}{2}$ . The Equation 2.1 can be simplified:

$$r_s = \frac{\sum_{i=1}^n x_i y_i - \frac{n(n+1)^2}{4}}{\sqrt{\sum_{i=1}^n x_i^2 - \frac{n(n+1)^2}{4}} \cdot \sqrt{\sum_{i=1}^n y_i^2 - \frac{n(n+1)^2}{4}}} \quad (2.2)$$

With this formula the rank correlation coefficient can be calculated in Libre Office Calc. First, the data were time normalized in Simi Motion. Thus the data points from Simi Motion and Simi Shape were comparable. Accordingly the data can be exported and further expressed. The x-coordinates of analyzed variables for markers and all four setups are at the beginning. The ranking is calculated for all five columns by the aid of the excel function =  $RANG(B2; B2:B101; 1)$ . The ranks of the two variables, between which the correlation is to be calculated, must be

multiplied. Furthermore the  $ranks^2$ , sum of each column and the help formula  $\frac{n(n+1)}{2}$  are required. Subsequently Spearman's correlation coefficient can be calculated for each axes. Figure 2.7 shows a calculation exemplary. In cells L103, P103 and Q103 the sum is represented. The higher the value for  $r_s$  the stronger the connectedness between the two variables.

L	M	N	O	P	Q	R
Product of the ranks Marker - 8 Cameras	Produ ▶	Produ ▶	Product of ▶	Rank Marker <sup>2</sup>	Rank 8 Cameras <sup>2</sup>	Rank 6 Cam ▶
338258	338230	338278	338277	338350	338350	338350
			n(n+1)/2	255025		
	r		=(L103-P105)/((P103-P105) <sup>0,5</sup> *(Q103-P105) <sup>0,5</sup> )			

**Figure 2.7:** Calculation of Spearman's correlation coefficient in Libre Office calc

In order to interpret and evaluate correlation coefficients, a classification must be made. In literature there is no uniform classification. In year 1980 Cohen made the following classification:

$r_s$	Interpretation
0,1	weak correlation
0,3	average correlation
0,5	strong correlation

**Table 2.1:** Cohen's classification

The classification as shown in Table 2.1 is not suitable for this question. In this study, it is anticipated that the correlation between the two variables is very high, because two different tracking processes are compared within the same movement. The following classification has been made and is adapted from several sources [14, 6].

$r_s$	Interpretation
$\leq 0,5$	weak correlation
0,5-0,8	average correlation
$\geq 0,8$	strong correlation

**Table 2.2:** Classification of correlation coefficient

The correlation coefficient is a suitable variable to evaluate the data. Angle range and average of the angle difference are unsuitable further statistical dimensions.

**Problem of angle range:** Angle range is calculated for marker based and silhouette based tracking with *highest value - lowest value*. Individual aberrations caused by tracking errors lead to a high angle range. This dimension is not resistant against mistakes and therefore non qualified.

**Problem of the average of angle difference:** Angle difference is determined for each moment and the mean value over all angle differences was calculated. A high mean value does not always mean a bad markerless tracking. It might just be caused by a constant offset which can occur because of differently defined coordinate systems in the Motion and the Shape model

**Standard deviation of angle difference:** This value states the distribution around an average.

The correlation coefficient and the standard deviation of angle difference are the most important values to evaluate the accuracy of markerless tracking with less cameras against marker based tracking with eight cameras. The correlation coefficient determines how consistent the angle progresses are, not regarding the exact values, e.g. amplitudes. The standard deviation shows how consistent the angle differences are. For example, consistent angle progressions of markerless and marker based data with highly different amplitudes cause a very high correlation and a high standard deviation of angle difference. That is why these two statistical values were used for further evaluation.

The position of the joint center is calculated from the x-,y- and z-coordinate. Therefore the absolute value, or even the length, of the vector have to be calculated of:  $\sqrt{x^2 + y^2 + z^2}$ . This indicates the level of the joint center in the coordinate system.

# 3 Results

In the following chapter, the results of the comparison between marker based and markerless tracking with less cameras will be presented. Five different movements were recorded. But for the analysis *running* was divided into *small steps* and *large steps* and *jumping* into *both legged jump*, *right legged jump only* and *left legged jump only*. So in fact there are eight different movements. The tracking results of flexion and extension movements are generally good. For the COM and the resulting velocity and acceleration of segment COM the results for all movements are also good. In the following part some movements will be described in detail. In the appendix all results and tables are listed. The correlation coefficient is relating to marker based data.

## 3.1 Influence of model initialization to tracking results

The model initialization has a significant influence on the accuracy of the data. There are three possibilities to adjust a model. First, there is the function of automatic fitting. When eight cameras are used this option is very reliable. Second, the function of optimizing joints. The last possibility is to fit the model manually. Due to the fact that automatic fitting works only well with eight cameras the difference between the other functions were tested for the *jump*. The initialization pose was tracked for six and four cameras. The correlation coefficient between automatic and manual adjustment was highest at both six and four cameras. The function *optimize joints* does not supply good results for this example. Figure 3.1 shows the different adaption options for the knee. As a result the models have been adjusted manually.

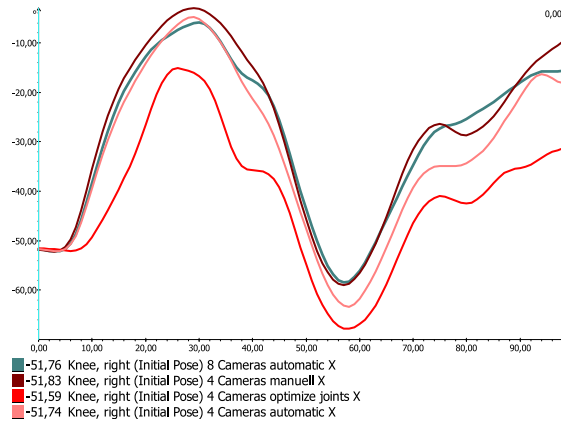


**Figure 3.1:** Comparison between the different adaption options for the initialization with four cameras for the right knee  
 dark red: manual, red: optimize joint, light red: automatic, blue: automatic eight cameras

## 3.2 Results of joint angles

### 3.2.1 Jump: both legged

#### Problems of marker less tracking

During the both legged jump problems occur in the right elbow. When the silhouette appearance barely changes during segment rotation it comes to problems. This can affect elbow angles as the elbow is performing a hyperextension instead of a flexion. If the arm is strongly rotated in the shoulder joint, very high negative correlations occur. Very high standard deviation of angle differences are the consequences (cf. Table A.4). Figure 3.2 shows the curve of the right elbow joint during the both legged jump. It has been noticed that the data is very similar but symmetrical to the x-axis. The arm is rotated in the shoulder so the correlation coefficient of the shoulder is also negative during an internal/external rotation.

#### Problems using less cameras

Also the pelvis segment is difficult to track because of its nearly rotationally symmetric shape and by that hip angles are affected. As seen in Figure 3.3 the pelvis rotates. The problems occur only when using three cameras. The correlation coefficient is still good, but the standard deviation of angle difference is very high caused by very high amplitudes. Tracking with eight, six and four cameras leads to a standard deviation in the range of  $7 - 10^\circ$ . When tracking with three cameras the standard deviation of angle difference is merely up to  $30 - 38^\circ$  (cf. Table 3.1).



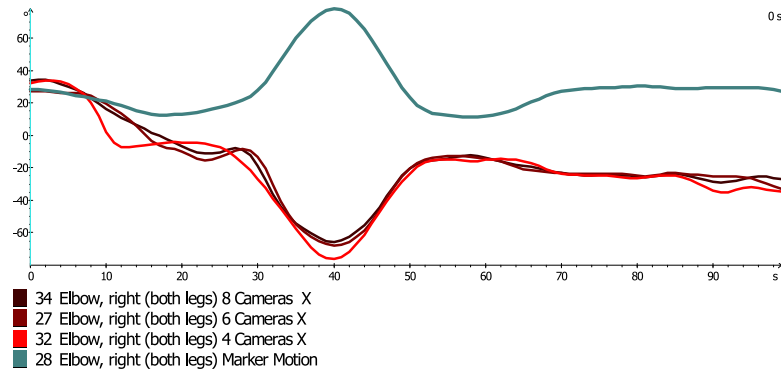
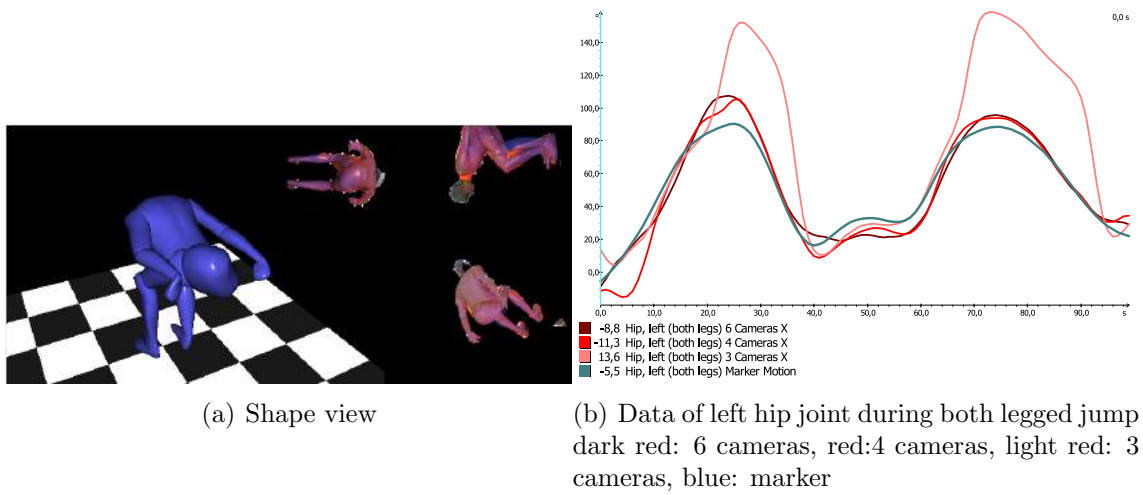


**Figure 3.2:** Data of right elbow during a flexion/extension movement  
dark red: 8 cameras, red: 6 cameras, light red: 4 cameras, blue: marker



(a) Shape view

(b) Data of left hip joint during both legged jump  
dark red: 6 cameras, red: 4 cameras, light red: 3 cameras, blue: marker

**Figure 3.3:** Rotation of the pelvis during tracking with three cameras and the effect of the amplitudes

Joint	Camera no	Flexion/Extension	
		correlation (l/r)	SD of angle diff. [°] (l/r)
Hip	8	0.976 / 0.977	7.063 / 5.761
	6	0.957 / 0.958	7.901 / 5.716
	4	0.965 / 0.969	9.455 / 7.480
	3	0.911 / 0.874	30.647 / 38.834

**Table 3.1:** Extract from: Table A.4 correlation coefficient & SD of angle difference from the hip at flexion/extension

### 3.2.2 Jump: right leg only

#### Problems of marker less tracking

When comparing the correlation coefficient, good results can be achieved for the shoulder. The standard deviation of angle difference is very high caused by very

high amplitudes (cf. Table 3.2). This is because the models are based on different standards. Therefore the shoulder joint is defined on a different place. Figure 3.4 shows a 3D figure with superimposed coordinate systems. The coordinate system is the local one with the origin in the center of gravity of segment. The two coordinate systems attack at different points as seen in Figure 3.4. The blue coordinate system is based on the markers and the red one on markerless data.

Joint	Camera no	Flexion/Extension	
		correlation (l/r)	SD of angle diff. [ ° ] (l/r)
Shoulder	8	0.919 / 0.975	10.43 / 15.21
	6	0.890 / 0.968	11.12 / 13.89
	4	0.824 / 0.977	13.56 / 13.75
	3	0.774 / 0.936	12.24 / 15.19

**Table 3.2:** Extract from: Table A.5 correlation coefficient & SD of angle difference of the shoulder at flexion/extension

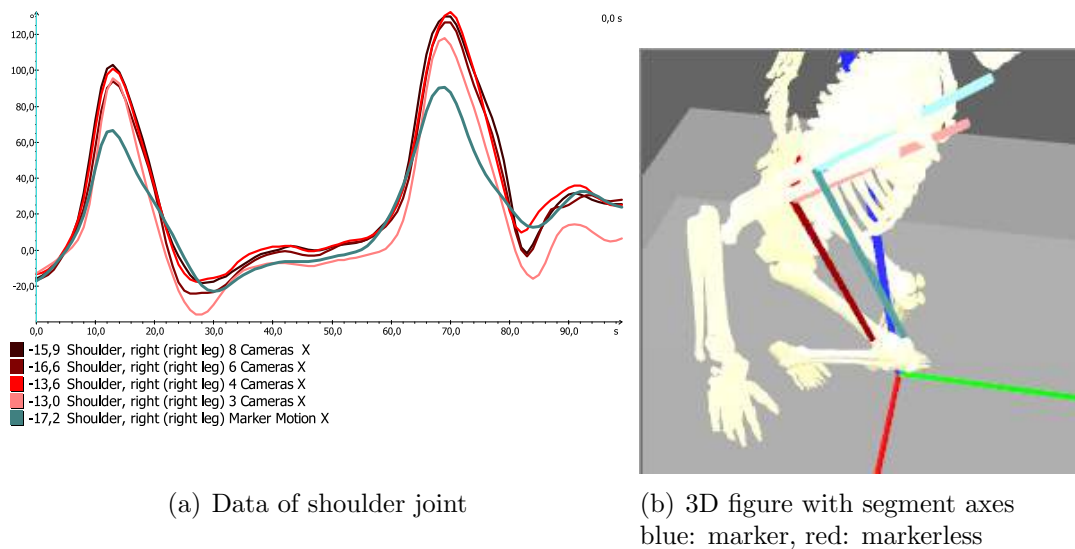


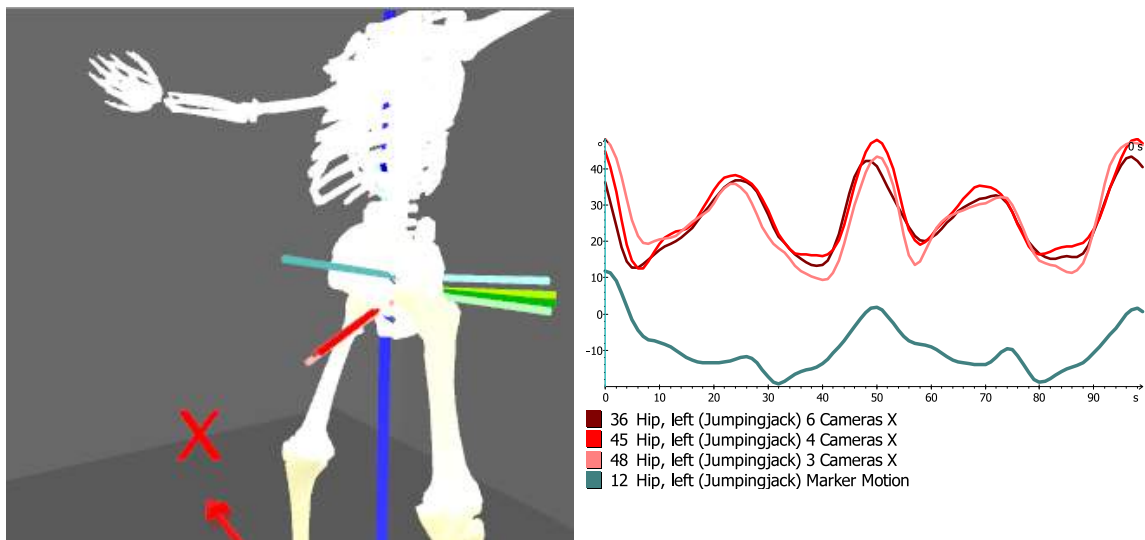
**Figure 3.4:** Different located joint centers and the influence of the amplitudes

### 3.2.3 Jumping-Jack

Only the lower extremities were analyzed in this example. The main movement was executed in the frontal plane and not in the sagittal. Therefore bad results were achieved for flexion and extension movements in the hip but good results for abduction/adduction.

#### Problems of marker less tracking

The shape of the pelvis is a problem as explained before in 3.2.1. It may happen that the pelvis tilts. Figure 3.5 shows superimposed 3D figures with the segment axes. The blue axis based on markers is straight and the red axes based on markerless data of six, four and three cameras are tilt. The consequence of this is a curve which is shifted on the y-axis. But the correlation coefficient is also not good, this leads to the very unstable tracking process. The model is readjusted in each frame so that there is a constant movement. Poorly adjusted models have a higher variability. There are also bad correlations for the rotation of the pelvis. A rotated thigh is the reason. Another superimposed 3D figure is seen in Figure 3.6. This time the segment axes of the thigh are shown. For the right thigh the segment axes of marker based and markerless data are pointed in the same direction. The coordinate systems of the left side differ from one another. The correlation coefficient for left hip is really bad (cf. Appendix Table A.9).



(a) Tilt pelvis and segment axes  
blue: marker based, dark: 6 cameras,  
normal: 4 cameras, light: 3 cameras

(b) Data of left hip  
blue: marker based, dark red: 6 cameras,  
red: 4 cameras, light red: 3 cameras

**Figure 3.5:** Tilt pelvis and the effect on the data of the left hip

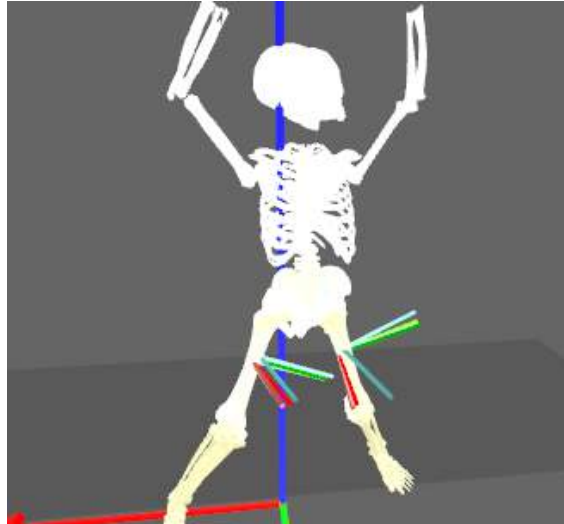


**Figure 3.6:** 3D figure and the segment axes of the thigh  
 blue: marker, dark red: 6 cameras, red: 4 cameras, light red: 3 cameras

### 3.3 Results of 3D joint position accuracy

#### 3.3.1 Average of segment velocity and acceleration over all movements

In this study attention is paid to the COM and the resulting variables as the velocity and acceleration of segment COM. For those variables consistently good results are obtained. Figure 3.7 shows the effect on the accuracy compared between eight, six, four and three cameras for the velocity and acceleration. The red line on the level of  $r_s = 0.9$  illustrates which setup achieved good results. When looking at the velocity it is evident that the camera setups with eight, six and four cameras provide high correlation coefficients. Only the camera setup with three cameras provides correlation coefficients under  $r_s = 0.9$  for lower arm and upper leg. This is not a bad result, but noticeable. When looking at the acceleration, similar results can be achieved. For three cameras the correlation coefficient of the arm and leg is under  $r_s = 0.9$ . But not only with three cameras, also for six and four cameras the correlation coefficient may be under  $r_s = 0.9$  in some cases.

**Velocity:** The averages over all movements and all segments are above  $r_s = 0.9$  for each setup (cf. Figure 3.8) even when some single values were below. On average good results can be achieved with all setups. It is important to note, that some segments achieve a lower accuracy (cf. Figure 3.7 (a)).

**Acceleration:** Only for three cameras the average over all movements and segments is below the threshold value as seen in Figure 3.9. It is also clearly visible, that the average differs even with six and four cameras caused by some values which are below (cf. Figure 3.7 (b)). In these diagrams it is clear that tracking with more

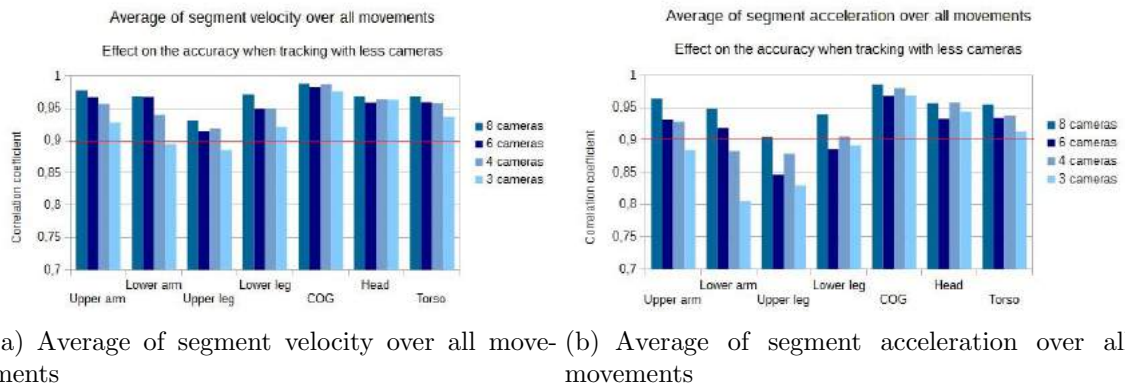


**Figure 3.7:** Effect on the accuracy when tracking with less cameras for each segment

cameras achieves higher accuracy.

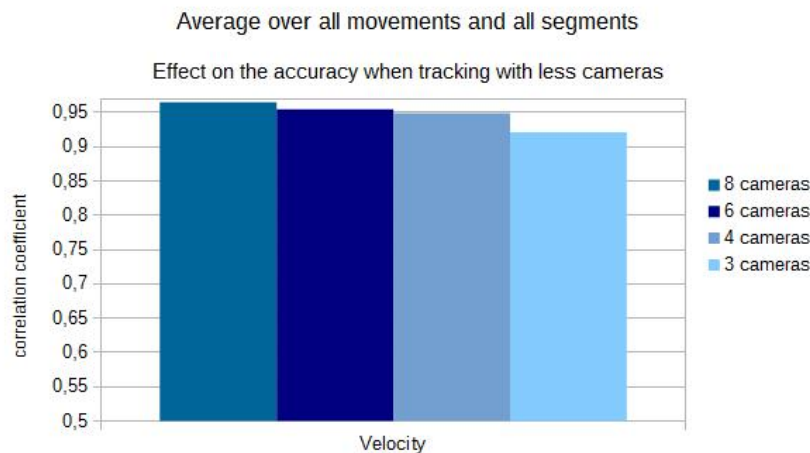


**Figure 3.8:** Average of correlation coefficient over all movements and segments

### 3.3.2 Segment center of mass of the movement Jump

When comparing the COM of marker based and markerless data, similar data can be achieved. Figure 3.10 shows the COM in the z direction of all jumps. There is a slight offset between the two data. The reason for that is the different calculation of the COM. The calculation of the markerless COM is based on the joint centers which are outputted from Simi Shape. The marker based COM is calculated from the markers which are attached on the body. So the marker based joint centers are above the markerless. Figure 3.11 shows an overview of the position of all joint centers. The dark blue joint centers represent the markerless data and the light blue ones the marker based data. The COM (circle in the middle of the body) is also shown in Figure 3.11. The blue circle describes the COM based on markers and the red one based on markerless data. It has been noticed that the joint centers in the

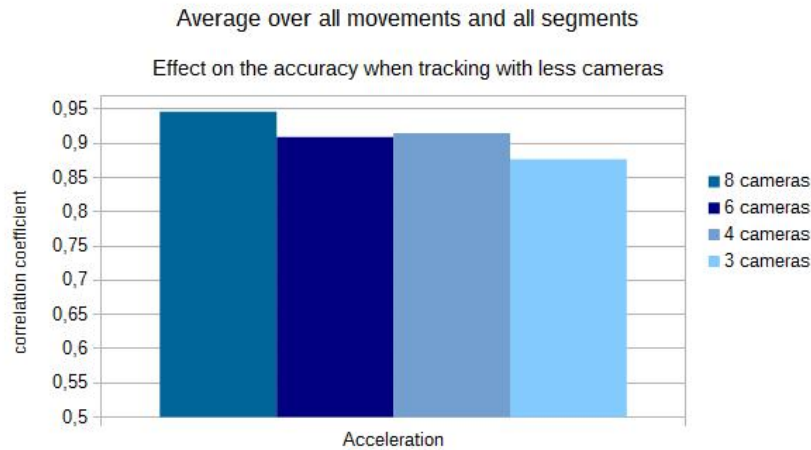


**Figure 3.9:** Average of correlation coefficient over all movements and segments

lower extremities are on the same level. Only in the upper body a shift upwards of marker based data can be observed. Due to the greater mass from the upper body the COM moves up. The correlation coefficient of the position of each joint center is really good and is about  $r_s = 0.97$ . But the slight offset can also be seen in the distance of the vectors. The difference between the markerless and marker based joint centers is in average 6cm (cf. Table A.3).

### 3.3.3 Segment velocity and acceleration of the movement

#### Jump

The segment velocity and acceleration can be calculated from the segment COM. The interpretation of the markerless data are noisier than the marker based data. But there is no direct influence on the correlation coefficient. Figure 3.12 shows the segment velocity of the right thigh during the both legged jump. When tracking with three cameras (light red graph) the data shows more deviation. This is confirmed by the correlation coefficient (cf. Table 3.3). A correlation coefficient of  $r_s = 0.848$  can be achieved for both legged jump. Looking at the average a minor deviation for tracking with three cameras can be found. This is the only setting with a correlation coefficient under  $r_s = 0.9$  (cf. Table A.1, A.2).

There is a mathematical relationship between the velocity and acceleration. The corresponding formula is  $a = \frac{dv(t)}{dt}$ . An error in the velocity propagates in the acceleration and raises to higher power. The data of the acceleration should have a lower value than the velocity data. Looking at Table A.1 and A.2 this is true. The data of the velocity is very noisy at the beginning and towards the end. So the error rate is very high in this range. When looking at the acceleration the data has to be noisier there. Figure 3.12 shows the acceleration of the right thigh. As it was expected the data is noisier. A high correlation is still determined.

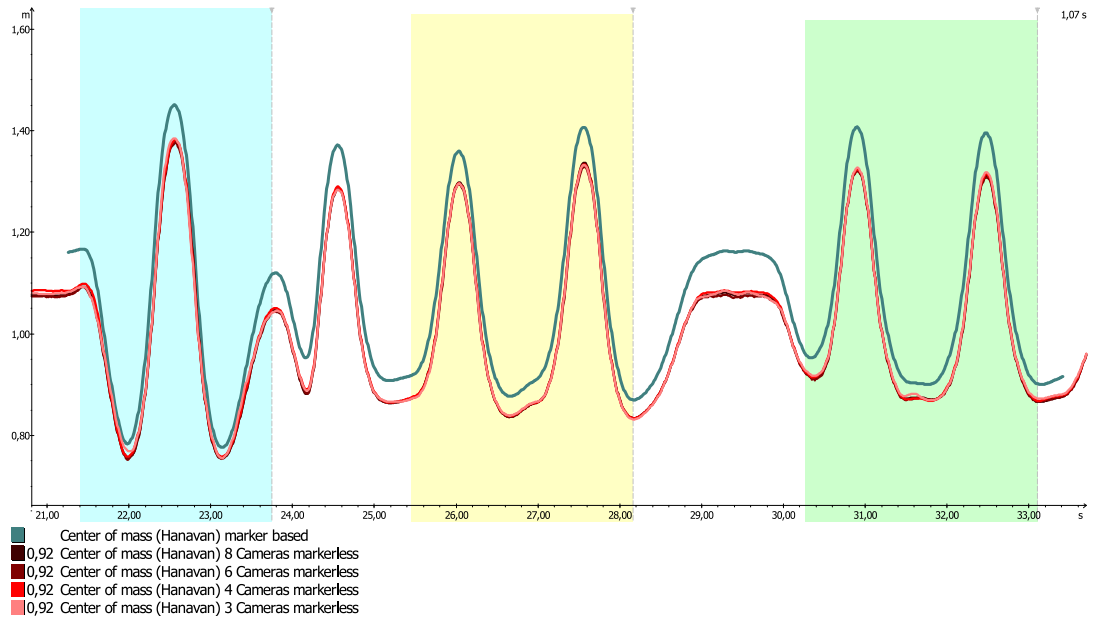


**Figure 3.10:** Data of the center of mass during the jump

Highlighted in blue: both legged, highlighted in yellow: right leg only, highlighted in green: left leg only  
 blue line: marker, dark red line: 6 cameras, red line: 4 cameras, light red line: 3 cameras

Segment velocity		
Joint	Camera no	correlation (l/r)
Upper leg	8	0.953 / 0.949
	6	0.930 / 0.907
	4	0.927 / 0.933
	3	0.833 / 0.848

**Table 3.3:** Correlation coefficient of segment velocity of the upper leg

The mean value in the tables of segment velocity/acceleration and location of the joint center is only made up of: Running (small/large steps), Jumping (both legged, right legged only and left legged only) and Kick boxing. The data of cycling and jumping jack are not included.

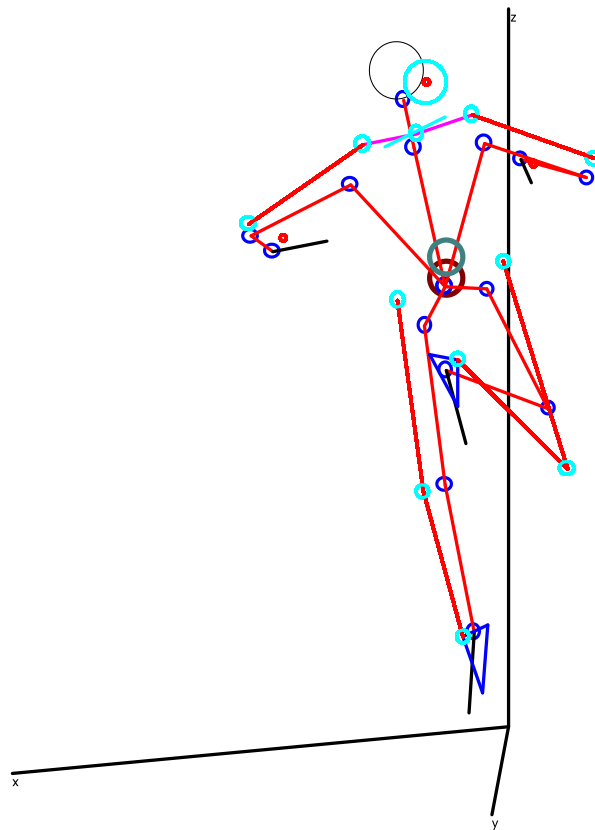
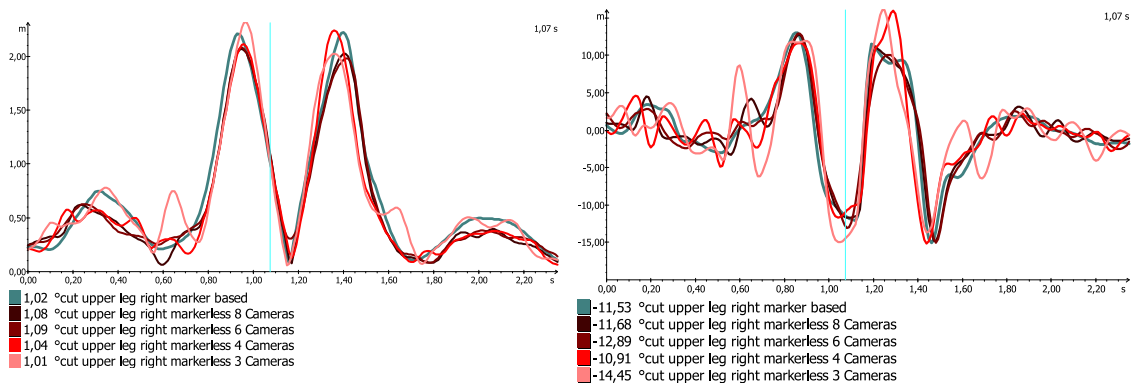


**Figure 3.11:** 3D Stick diagramm: marker based joint centers (light blue) vs. silhouette based (dark blue)  
Center of gravity: blue: marker based, dark red: 8 cameras markerless



(a) Velocity of the right thigh  
blue: marker, dark red: 6 cameras, red: 4 cameras, light red: 3 cameras

(b) Acceleration of the right thigh  
blue: marker, dark red: 6 cameras, red: 4 cameras, light red: 3 cameras

**Figure 3.12:** Comparing velocity and acceleration of the right thigh



## 4 Summary

In the following chapter the above-mentioned results are summarized again. It discusses the problems arising during the process of marker less tracking. Furthermore there is a short outlook about unused functions in Simi Shape. The average over all movements and right/left was calculated to have a clearer view on the results. The complete table is annexed (cf. Table A.12).

There are some settings which are not used in this study and have not been studied yet. E.g. the function of *Motion constraints*. This function prevents the model from taking unrealistic poses. With a higher weighting the elbow angle could be improved. Also the effect of *iterations per frame (ipf)* should be evaluated more closely. This function describes how often the model is adjusted in one second to the actual pose. In this work, all markerless tracking were performed with a tracking parameter of 10 ipf. The influence of different settings (e.g. 15 ipf) on data accuracy should be tested. It should be noted that the tracking time slows down. When comparing the COM of markerless and marker based tracking a slight off-set can be seen. The main problem is the calculation of the COM. Another weighting of the parameters in the calculation should be tested.

The aim of this study was to evaluate the accuracy of markerless tracking against marker based tracking with less cameras. The problem of the rotated arm can be seen in all trials. Therefore the average of correlation coefficient of the elbow is bad. The values close to  $r_s = 0$  arise through the difference between right and left. Either the results for the right or left elbow are bad. Apart from the bad results in the elbow there are good results for the other joints. The correlation coefficient of the hip (flexion/extension) can still achieve good results for eight, six and four cameras. Only for three cameras the correlation coefficient is moderate. During an adduction/abduction and rotation good results can not be achieved for each setup. When increasing the camera number, the correlation coefficient reaches higher values. A significant increase in the accuracy between marker based and markerless data of six and eight cameras is not reached. The difference between six and four/three cameras is significantly higher. The results differ from each other by more than  $r_s = 0,05$  which corresponds to a value of 9%. By using two markers the results can be improved. This has already been proved in the previously cited study [2].

Joint angles are insignificant in most sports. Importance is attached to the COM, the velocity and acceleration of segment COM. Good results can be achieved in this area for all setups even for tracking with three cameras. It must be remembered that

---

the tracking process with three cameras is much more difficult. The model can lose the silhouette and needs to be adjusted more often. The effort to achieve acceptable results is much higher. To get a good balance between effort and camera number, four cameras should be used. In clinical issues using only four cameras is not recommended. It is not possible to make a correct bio mechanical statement about some joint angles. As a further excitation, it is also conceivable to use some additional markers to improve the accuracy and to avoid the rotation within the segments. A minimum of three markers can prevent segment rotation. A sensible arrangement of the cameras must be considered as 3D-coordinates can only be calculated if each marker is seen in at least two cameras for every moment. An interesting question for further investigation is how the accuracy between marker based and markerless data varies from one day to another measuring of the same subject. The markers have to be attached every day again, which could lead to errors. The model can always be reused.

## **Part III**

# **Effects on markerless 3D joint position accuracy using GoPro<sup>®</sup> cameras**

# 5 Expanded Basics

## 5.1 Technical Equipment

In the following part, the type of cameras, which were used in addition will be presented. The problems and differences to high-speed cameras will also be discussed.

### GoPro® cameras

Four GoPro® Hero 3 cameras were used. Three of the white edition and one of the black edition. The difference between the two models is, that the GoPro® Hero 3 black can record videos in other resolutions. It has to be filmed at the same resolution and frame rate in order to evaluate the data. They acquire videos with a maximum frame rate of 60Hz and a resolution of 1280x720 pixels. The field of view is ultra wide, which corresponds to 170°. Another important parameter for cameras is the shutter speed. The shorter the shutter speed, the better fast movements can be recorded. The shutter speed of GoPro® cameras is 1/8192s as a minimum and not continuously adjustable. In contrast to the GoPro® cameras the shutter speed of high speed cameras can be adjusted.

3D data can only be calculated if the video from each camera starts at the same time and runs at the same frequency. GoPro® cameras can be triggered by a Smart Remote from GoPro® via wireless, although the recording starts slightly delayed. A common start frame can be set in Simi Motion for each camera.

Due to the strong fish eye effect, the recordings are highly distorted. A distortion correction should be made with a chessboard to avoid this effect. Figure 5.1 shows the difference between a distorted and an undistorted image. The distortion correction has to be made only once for each camera and can then be reused unless there are changes to the settings such as field of view. If the distortion is not rectified, this could lead to incorrect 3D data.



(a) distorted illustration

(b) undistorted illustration

**Figure 5.1:** Comparison between distorted and undistorted illustration

Ring lights can not be attached to GoPro<sup>®</sup> cameras thus retro reflective markers cannot reflect. For this reason calibration has to be carried out with LED markers. Due to the very slow shutter speed, the calibration wand has to be moved very slowly. Otherwise, the markers are no longer displayed as a circle but rather than an oval.

The software is not able to identify an oval as a marker which leads to less raw data for a sufficient calibration. The distortion correction has to be applied to the calibration videos before corrected raw data can be calculated in order to subsequently calculate the calibration. The standard deviation of the wand length is higher in comparison to the high-speed system (cf. section 1.1). At the time of execution, there was no LED wand with very bright LEDs, which are needed for recognition in bright environments with the GoPro<sup>®</sup>. Because of the encountered difficulties, the reliable but extensive method of manual calibration has to be used.

Pictures were taken at the same time by all GoPro<sup>®</sup> cameras with a wand standing upright at various points. In the simplest case, four positions are chosen, which subsequently form the corners of a cube. The exact distance between the positions and the length of the wand must be known. Using this data a calibration system can be build. Figure 5.2 shows the used calibration system. The first four points are the lower corners of the cube. Points E, F, G and H are the upper four corners with the length of the wand as the z-coordinate. It must be ensured that a right-handed coordinate system is created. This way of calibrating the GoPro<sup>®</sup> is the easiest way, because no problems can arise and only four pictures or short videos are needed. With the normal wand calibration it is very likely that not enough raw data are available and therefore the calibration fails.

X [m]	Y [m]	Z [m]	Bezeichnung
0,0000	0,0000	0,0000	A
1,7900	0,0000	0,0000	B
1,7900	1,1300	0,0000	C
0,0000	1,1300	0,0000	D
0,0000	0,0000	1,0400	E
1,7900	0,0000	1,0400	F
1,7900	1,1300	1,0400	G
0,0000	1,1300	1,0400	H

**Figure 5.2:** Used calibration system

Unlike with the high-speed system, there is no live view at GoPro<sup>®</sup> cameras. All recordings have to be made before the calibration can be checked for accuracy. The video files are transferred to the PC using an USB cable.

## 5.2 Image processing

In the following section, the image processing is explained in detail. These essentials are used in order to make an accurate statement about which settings (e.g frame rate, shutter speed) are required for sports recordings. All data used can be found in the data sheets of the corresponding camera [9, 10, 1].

### 5.2.1 Theoretical bases of optics

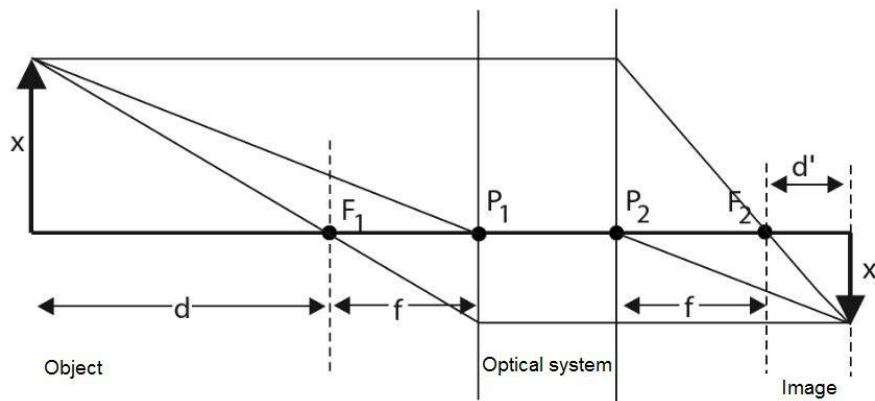


**Figure 5.3:** schematic, simplified optical path through a lens [11, p. 87]

Figure 5.3 shows a schematic, simplified optical path through a lens. The  $x$  in the figure denotes the object size, the  $d$  the distance between the object and the lens, and the  $f$  the focal distance. It is clearly visible, that the size  $x'$  of the object is displayed much smaller on the sensor, provided  $d$  is greater than  $f$ . The lateral projection level  $m_L$  describes the ratio of image size  $x'$  to object size  $x$ . This results in the formula:

$$m_L = \frac{x'}{x} = \frac{\Delta x'}{\Delta x} = \frac{f}{d} \quad (5.1)$$

Each camera includes a sensor chip with a specific resolution and size. With these values the real pixel size on the sensor can be calculated. The size  $\varepsilon$  of one pixel is known. Therefore the object size on the chip  $x'$  in mm can easily be converted to the size in px. The pixel shift from one frame to the other can be calculated. If the displacement is too large, a tracking with the software Simi Shape can be very difficult.

### 5.2.2 GoPro<sup>®</sup> cameras

At GoPro<sup>®</sup> cameras it is not possible to adjust the shutter speed. This is a defining factor in the evaluation of sports recordings. To prevent a blurring of the movement,

recordings should be taken with the shortest possible shutter speed. Figure 5.4 shows an image section of a fast movement. The arm can not be displayed correctly and the contours are blurred. For Simi Shape it is not possible to find a hard contour to perform a good segmentation in order to fit the model into the silhouette.

There are several variables affecting the calculation of pixel offset. Frame rate ( $f_R$ ) and resolution are the only mutable variables at GoPro<sup>®</sup> cameras, the others are constant. But frame rate and resolution are directly related, the higher the frame rate, the lower the resolution. The velocity ( $v$ ) of the movement is also crucial for the calculation and is measured as a covered distance per unit of time. The GoPro<sup>®</sup> camera takes 60 frames per second. For the calculation it is important to know how many meters are covered from one frame to the next. GoPro<sup>®</sup> cameras were conceived for high quality video material. The ISO value indicates how light-sensitive the sensor of the camera is. Small values reflect a low light sensitivity. GoPro<sup>®</sup> cameras want to keep the ISO value as low as possible and thus the shutter speed is maximized in order to get a well exposed image. This is why the shutter speed ( $t_s$ ) is assumed as  $\frac{1}{f_R}$  and therefore the covered distance is  $x = \frac{v}{f_R}$ .



**Figure 5.4:** Blurring arm during a too fast movement

$$x' = \frac{v}{f_R} * \frac{f}{d} \quad (5.2)$$

The chip installed in GoPro<sup>®</sup> cameras has a higher resolution than the one used for recording the video data. The ratio of resolution to dimensions of the chip should therefore be considered in the formula.  $X_c$  is the dimension of the chip, and  $q$  is the resolution of the video.

$$x' = \frac{\frac{1}{\varepsilon} * \frac{f}{d} * \frac{v}{f_R}}{\frac{X_c}{q}} \quad (5.3)$$

After dissolving the double fraction:

$$x' = \frac{q * f}{\varepsilon * X_c} * \frac{v}{d * f_R} \quad (5.4)$$

**GoPro® Hero 3 White edition**

pixel size $\varepsilon$	focal distance $f$	distance $d$	velocity $v$	frame rate $f_R$	resolution
$2.2 \frac{\mu\text{m}}{\text{px}}$	3 mm	2 m	$7 \frac{\text{m}}{\text{s}}$	60 Hz	1280 px $\times$ 720 px

**Table 5.1:** Example parameter GoPro® Hero 3 White edition

The highest frame rate of 60 fps, is recorded at a resolution of 1280x720px. The chip size is 2592x1944px. Because the movement is carried out in the vertical direction of the image, the variables  $X_c$  and  $q$  of the chip are as follows:  $X_c = 1944$  px and  $q = 720$  px.

$$x' = \frac{720 \text{ px} * 3 \text{ mm}}{0.0022 \frac{\text{mm}}{\text{px}} * 1944 \text{ px}} * \frac{7000 \frac{\text{mm}}{\text{s}}}{2000 \text{ mm} * 60 \text{ Hz}} = 29.46 \text{ px} \quad (5.5)$$

A shift by 29 px corresponds to an offset of about 4% per frame. As seen in Figure 5.4, the arm is greatly blurred.

**GoPro® Hero 4 Silver edition**

The GoPro® Hero 4 camera is the latest model of GoPro®. There are higher frame rates adjustable, but the shutter speed cannot be adjusted manually either. The size of the chip is higher with a dimension of 4000x3000px. It is crucial that the size of the chip is larger at the GoPro® Hero 4 camera. Some tests could be performed with this camera, to test whether a higher frame rate may provide better results. Three shots were taken with different settings.

pixel size $\varepsilon$	focal distance $f$	distance $d$	velocity $x$	frame rate $f_R$	resolution
$1.55 \frac{\mu\text{m}}{\text{px}}$	3 mm	2 m	$7 \frac{\text{m}}{\text{s}}$	240 Hz	848 px $\times$ 480 px

**Table 5.2:** Example parameter GoPro® Hero 4 Silver edition: 240fps

240fps can be taken with a resolution of 848x480px. The used high-speed cameras record in a similar resolution, which would therefore be sufficient. During the tests the movement was performed in the vertical direction.

$$x' = \frac{480 \text{ px} * 3 \text{ mm}}{0.00155 \frac{\text{mm}}{\text{px}} * 3000 \text{ px}} * \frac{7000 \frac{\text{mm}}{\text{s}}}{2000 \text{ mm} * 240 \text{ Hz}} = 4.51 \text{ px} \quad (5.6)$$

As shown in Figure 5.5, the arm is still clearly displayed with hard contours, because the offset from one frame to the next is only about 1%.





**Figure 5.5:** 240fps at a resolution of 848x480px, not blurred

pixel size $\varepsilon$	focal distance $f$	distance $d$	velocity $x$	frame rate $f_R$	resolution
$1.55 \frac{\mu\text{m}}{\text{px}}$	3 mm	2 m	$7 \frac{\text{m}}{\text{s}}$	120 Hz	1280 px $\times$ 720 px

**Table 5.3:** Example parameter GoPro<sup>®</sup> Hero 4 Silver edition: 120fps

120 fps can be taken with a resolution of 1280x720px.

$$x' = \frac{720 \text{ px} * 3 \text{ mm}}{0.00155 \frac{\text{mm}}{\text{px}} * 3000 \text{ px}} * \frac{7000 \frac{\text{mm}}{\text{s}}}{2000 \text{ mm} * 120 \text{ Hz}} = 13.54 \text{ px} \quad (5.7)$$

The movement is no longer displayed with a frame rate of 120fps. It is blurred, because the pixel offset is already too large. Although the offset is approximately 2%. Figure 5.6 shows the examined movement.



**Figure 5.6:** 120fps at a resolution of 1280x720px, blurred

pixel size $\varepsilon$	focal distance $f$	distance $d$	velocity $x$	frame rate $f_R$	resolution
$1.55 \frac{\mu\text{m}}{\text{px}}$	3 mm	2 m	$7 \frac{\text{m}}{\text{s}}$	60 Hz	1920 px $\times$ 1080 px

**Table 5.4:** Example parameter GoPro<sup>®</sup> Hero 4 Silver edition: 60fps

The GoPro<sup>®</sup> Hero 4 is able to record 60fps in a higher resolution than the GoPro<sup>®</sup> Hero 3.

$$x' = \frac{1080 \text{ px} * 3 \text{ mm}}{0.00155 \frac{\text{mm}}{\text{px}} * 3000 \text{ px}} * \frac{7000 \frac{\text{mm}}{\text{s}}}{2000 \text{ mm} * 60 \text{ Hz}} = 40.64 \text{ px} \quad (5.8)$$

The movement is, as it was already the case for GoPro<sup>®</sup> 3, blurred. A higher resolution does not help. The pixel offset is about 4%. Figure 5.7 shows the example.

The last two settings are unsuitable for tracking with Simi Shape. The background segmentation recognizes no sharp contours and allocates the blurred arm falsely to



**Figure 5.7:** 60fps at a resolution of  $1920 \times 1080px$  , very blurred

the background. This is because the lower threshold value is not exceeded, as explained before in subsection 1.3.2. Even without the option of adjusting the shutter speed, good results can be achieved by increasing the frame rate. For cost reasons, the following experiments were carried out only with a GoPro<sup>®</sup> Hero 3. It is conceivable that the results are more strongly correlated if a better action camera is used.

### 5.2.3 Basler Scout scA640-120gm

The used high-speed cameras can be variable set in the frame rate and the shutter speed ( $t_s$ ). For sport recordings the highest frame rate should be used in order to get good information. However, the shutter speed is crucial for the final result. This indicates how long the receiving sensor of the camera is exposed to light between each image. The shorter the shutter speed, the sharper the images. In the following section the influence on the image at three different shutter speeds was investigated. All other variables were constant. Figure 5.8 shows the influence of three different shutter speeds on the representation of the arm.

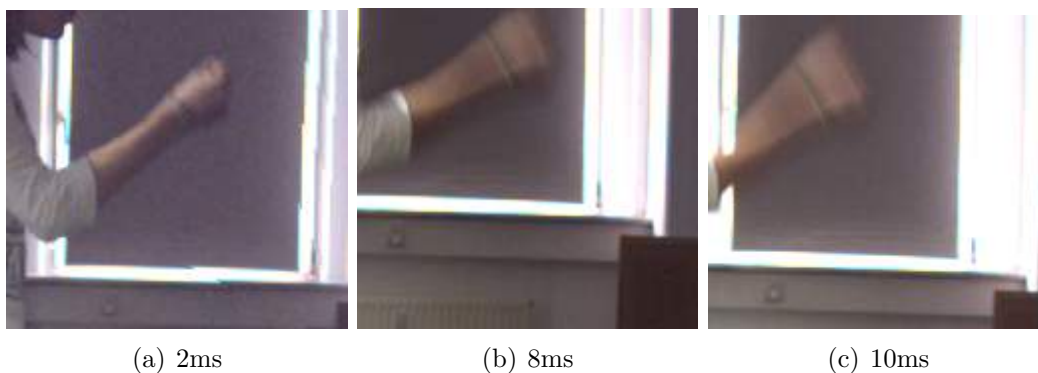


**Figure 5.8:** Comparison between three different shutter speeds

Contrary to the GoPro<sup>®</sup> cameras, the pixel offset is calculated with the shutter speed. For the calculation the covered distance within the shuttertime is needed, which is why  $x = v * t_s$ . The following formula calculates the pixel offset from one frame to the next.

$$x' = \frac{v * t_s * \frac{f}{d}}{\varepsilon} \quad (5.9)$$

After dissolving the double fraction:

$$x' = \frac{v * f}{\varepsilon * d} * t_s \quad (5.10)$$

The velocity  $v$ , focal distance  $f$ , pixelsize  $\varepsilon$  and distance  $d$  become a constant  $C$ :

$$x' = C * t_s \quad (5.11)$$

Now it is clear that the shutter speed is the only variability. Three shots were taken in which only the shutter speed was changed. The frame rate is fixed at 120fps.

pixel size $\varepsilon$	focal distance $f$	distance $d$	velocity $x$	shutter speed $t_s$
$5.6 \frac{\mu\text{m}}{\text{px}}$	7.8 mm	2 m	$7 \frac{\text{m}}{\text{s}}$	2 ms

**Table 5.5:** Example parameter High speed camera:  $t_s = 2$  ms

The first experiment was carried out with a shutter speed of 2ms. The arm is still clearly recognizable in this setting (cf. Figure 5.8 (a)). A pixel offset of 9,76 px per frame can be calculated with the help of Equation 5.11. If this is seen in relation to the absolute image size, an offset of 1,9% exists.

$$x' = 4875 \frac{\text{px}}{\text{s}} * 0.002 \text{ s} = 9.76 \text{ px} \quad (5.12)$$

pixel size $\varepsilon$	focal distance $f$	distance $d$	velocity $x$	shutter speed $t_s$
$5.6 \frac{\mu\text{m}}{\text{px}}$	7.8 mm	2 m	$7 \frac{\text{m}}{\text{s}}$	8 ms

**Table 5.6:** Example parameter High speed camera:  $t_s = 8$  ms

In the next experiment, the shutter speed was increased to 8ms. The arm is shown already blurred. The pixel offset is 39,05px per frame, this represents a value of 7,9%.

$$x' = 4875 \frac{\text{px}}{\text{s}} * 0.008 \text{ s} = 39.05 \text{ px} \quad (5.13)$$

pixel size $\varepsilon$	focal distance $f$	distance $d$	velocity $x$	shutter speed $t_s$
$5.6 \frac{\mu\text{m}}{\text{px}}$	7.8 mm	2 m	$7 \frac{\text{m}}{\text{s}}$	10 ms

**Table 5.7:** Example parameter High speed camera:  $t_s = 10 \text{ ms}$

In the last experiment, the shutter speed was 10ms. The arm is very blurry. The offset of 48,75px per frame corresponds to an offset of approximately 10%

$$x' = 4875 \frac{\text{px}}{\text{s}} * 0.01 \text{ s} = 48.75 \text{ px} \quad (5.14)$$

The last two settings are unsuitable for tracking with Simi Shape. The background segmentation recognizes no sharp contours and allocates the blurred arm falsely to the background. This is because the lower threshold value is not exceeded, as explained before in subsection 1.3.2. It can be assumed that a displacement of less than 2% is still clearly visible.

# 6 Expanded Methods

Based on the results of the previous part of this work, the effect on the accuracy of markerless tracking against marker based tracking with low quality cameras will be investigated. As a result of the previous part of this work, at least four cameras were recommended due to the lower effort and better accuracy. The experimental setup consists of two different camera systems. First, a high-speed system with eight cameras and secondly a system with four GoPro<sup>®</sup> cameras. Eight camera marker-based data is selected as reference. In order to apply the results of the first part of the work to athletic movements four camera high speed data was collected. Moreover the difference between high speed cameras and GoPro<sup>®</sup> cameras can better clarify if the same number of cameras were used. For the analysis this three data sets are used for comparison with the marker based data of eight cameras:

- **Eight cameras** markerless
- **Four cameras** markerless
- **Four GoPro<sup>®</sup> cameras** markerless

Three fast athletic movements were recorded in order to test the influence of the recording conditions (e.g shutter speed and frame rate). A mobile camera system, without any cables is suitable for athletic movements under competition conditions, which is why those movements were examined. As explained before GoPro<sup>®</sup> cameras are only conditionally suitable for very fast recordings.

In the following part the three different performed movements and the corresponding camera setups are explained.

## 6.1 Data capture setup using high speed and GoPro<sup>®</sup> cameras

Three athletic movements were recorded in a gym performed by a male person. In detail, there are three different throws: volleyball, handball and basketball. The basketball throw is a rather slow movement compared to the others. The top speeds of the wrist in volleyball and handball are about  $10 \frac{\text{m}}{\text{s}}$ , whereas only  $5 \frac{\text{m}}{\text{s}}$  are achieved in basketball. Figure 6.1 shows the marker speeds of the middle finger base joint of volleyball and basketball in comparison.

The movements were recorded with eight high speed cameras and four GoPro<sup>®</sup> cameras. As in the evaluation the number of cameras was reduced to four, the camera setup was chosen accordingly. The four remaining cameras have been placed

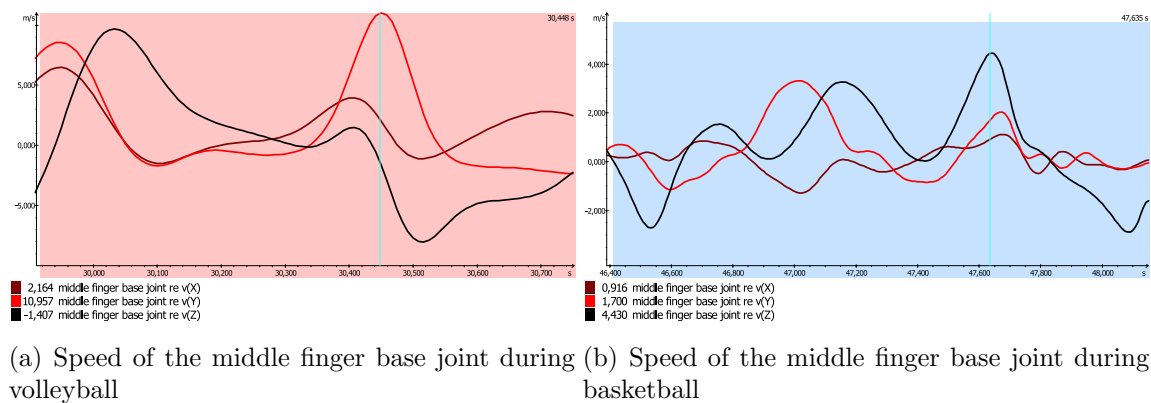


Figure 6.1

first, so that a good tracking would be possible. It has been kept to the recommendation from subsection 2.1.6. The four GoPro<sup>®</sup> cameras were similarly positioned. Certainly, the distance between subject and GoPro<sup>®</sup> cameras has to be chosen much less, in order to maximize the recorded details of action. With the other four cameras, a camera setup was created, allowing error-free marker based tracking. Figure 6.2 shows the used camera setup. Red circled cameras were used for the four camera setup.

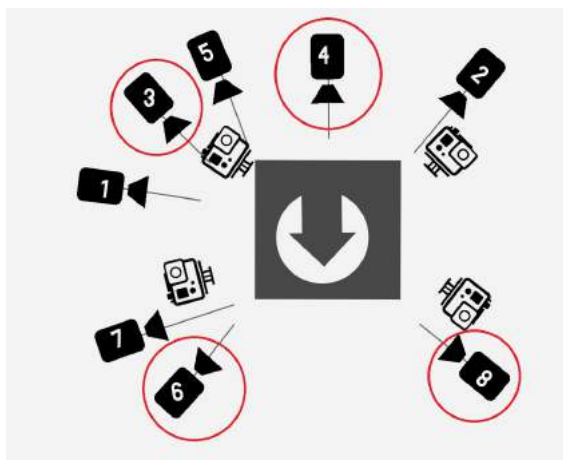
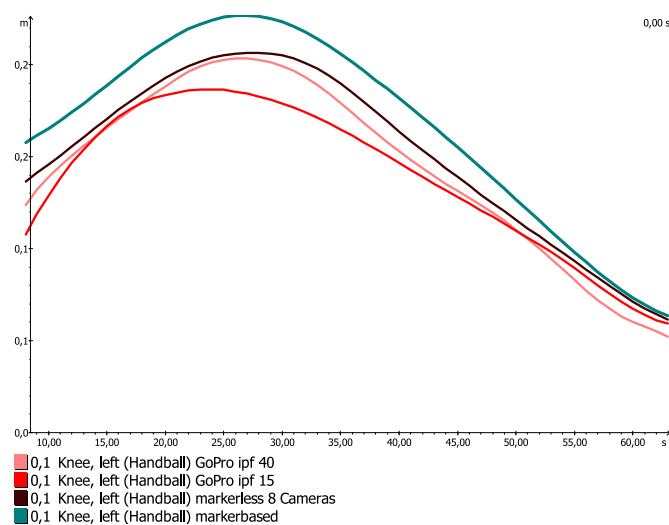


Figure 6.2: Camera setup in the gym. Red circled cameras: four camera setup

Evaluation and filtering of the data is carried out as already described in subsection 2.2.1 and 2.2.2. The focus of the evaluation was placed on the sporting aspects such as body center of mass, segment velocity and acceleration as well as position of joint centers. When tracking with Simi Shape one setting has been changed in comparison to the previous part. The *iterations per frame* was increased when tracking the data of the GoPro<sup>®</sup> cameras. This setting describes how many times per frame the model is adapted to the silhouette. This setting is by default 15 ipf and has not been modified for high speed cameras. For GoPro<sup>®</sup> cameras the value has been increased to 40 ipf. This is mainly because of the lower frame rate and the resulting

large variations from one frame to the next. The model needs more time to adapt better to the silhouette. The Handball throw was tracked with 15 ipf again to test whether the settings attracts noticeable changes. Figure 6.3 shows the data from the joint center of the left knee during handball throw. The light red line represents the data of the 40 ipf tracking and the red line of the 15 ipf tracking. A difference between the two graphs can be seen. In order to assess the changed data, marker based data and markerless data of eight high speed cameras can also be seen in the diagram. Increasing the ipf actually causes better data which are more closely to the high speed data. It should be noted that the computing power is greatly impaired. The tracking takes much longer.



**Figure 6.3:** Comparison between two GoPro<sup>®</sup> data with different ipf

## 6.2 Special problems when tracking with GoPro<sup>®</sup> cameras

If the GoPro<sup>®</sup> is calibrated manually and photos instead of short videos were taken, problems may occur. The GoPro<sup>®</sup> camera captures photos in a different resolution than videos. The positions of the pixels is out of sync, because a much larger area can be seen on the pictures. The Pictures need to be adapted in resolution and image area to the video. Figure 6.4 shows the comparison between the original image and the cropped image. The difference is seen especially in the height of the image. It is very important that the calibration is correct and the point in the calibration video is the same as in the movement video. With the help of the 3D still image measurement, this can be checked. The 3D still image measurement is the most common method in Simi Motion to check the accuracy of the calibration.

For all videos the same point is clicked, lines are projected in every video. If the lines intersect at the same point, the calibration is good.



(a) original image

(b) cropped image

**Figure 6.4:** Comparison between original and cropped image

Due to the different calibration methods, the coordinate system is set differently. In the normal wand calibration the origin of the coordinate system is set to the origin of the L-Frame. In the manual calibration the origin of the coordinate system is set in the point with the coordinates  $(0/0/0)$ . The model in Simi Shape is placed at the origin and all resulting data refer to this coordinate system. Since the coordinate systems were different, the data is loaded with an offset. In Simi Motion there is the possibility to move and rotate the coordinate system with the result that the data will fit together.

Another problem is the slight time offset when starting the cameras. Remedy can be easily created with an event. In this study, a ball was thrown to the ground at the beginning of the video. The videos of the GoPro<sup>®</sup> cameras were cut on that frame where the ball touches the ground.



# 7 Results

In the following chapter, the results of the comparison between marker based and markerless tracking with low quality cameras will be presented. Three different movements were recorded. In order to exclude the fault of a worse fitted model, the model was adapted well with eight cameras and used for the other setups. In the appendix all results and tables are listed. The correlation coefficient is relating to marker based data. Another value was calculated in order to assess the difference of the position of joint centers. The standard deviation of the mean difference between the vector has been calculated in addition.

## 7.1 Volleyball

Only the moment of the jump and the strike was crucial for the evaluation. In the following part all results that are important for an athletic evaluation are described.

### 7.1.1 Position of joint centers

When comparing the course of the various joint centers no significant difference is observed. All results are above  $r_s = 0.9$ . This corresponds, according to the classification made in Table 2.2, to a very good correlation. There is no significant difference between GoPro<sup>®</sup> cameras and high speed cameras. Merely at the exact position, a difference can be seen. Figure 7.1 shows a 3D stick diagram of the position of all joint centers. The light blue circles are the joint centers of the marker based data, the dark blue ones of markerless data with eight cameras, the dark red ones of markerless data with four cameras and finally the dark green circles represent the joint centers of markerless data with GoPro<sup>®</sup> cameras.

On closer consideration of the right knee a slight offset between marker based data (light blue) and markerless data recorded with high speed cameras (dark blue and red) can be seen. The joint centers of GoPro cameras (green) are even higher. The mean value of the deviation is about 3cm against 1cm (cf. Table 7.1). In addition, the standard deviation of this was calculated. This indicates how much the values fluctuate around the mean. A high standard deviation means a large irregularity in the data. The standard deviation of the GoPro<sup>®</sup> data are the highest.

In Figure 7.1 it can be seen that the right arm of the GoPro<sup>®</sup> data is very different to the others. As described in subsection 5.2.2 the representation of the arm is blurred due to the low shutter speed and frame rate. Therefore a tracking with Simi Shape was almost impossible. It is clearly seen in Table A.13 that the correlation in the right shoulder is rather poor. There is a peculiarity that affects the

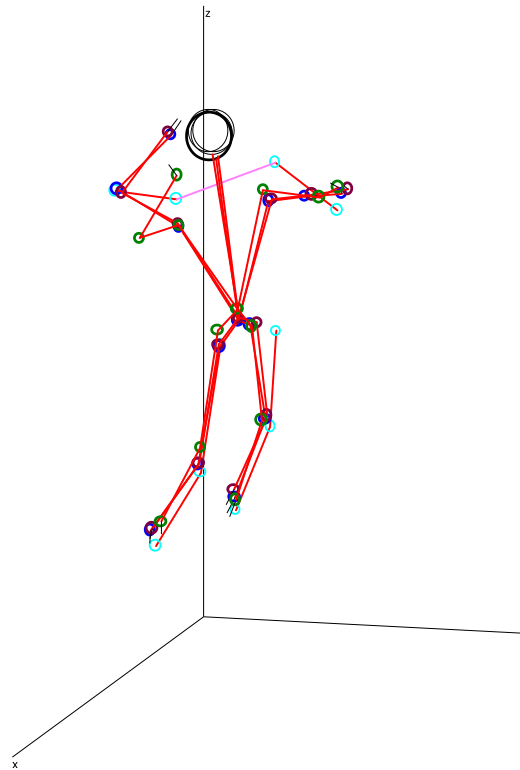


**Figure 7.1:** 3D Stick diagram: marker based joint centers (light blue) vs. markerless 8 cameras (dark blue); markerless 4 cameras (red) and markerless GoPro<sup>®</sup> (green)

Joint	Camera no	Position of Joint centers	
		mean deviation	SD of mean value(1/r)
knee	8	0.03 / 0.01	0.04 / 0.02
	4	0.02 / 0.01	0.03 / 0.02
	GoPro <sup>®</sup>	0.00 / 0.03	0.02 / 0.03

**Table 7.1:** mean deviation & SD of mean deviation from the joint centers of the knee

results. The shoulder is the most mobile human joint. Any movements of the arm are made of multiple joints from a joint group. An abduction is possible up to 180°, but only with the involvement of the shoulder girdle and the spine [5]. The model of Simi Shape is constructed of separate segments and there is only one segment for the upper body. A spine and shoulder girdle does not exist. The optical extension of the upper body can not be displayed and therefore the position of the shoulder joint center is strongly influenced.

## 7.1.2 Body center of mass (COM)

When calculating the COM, there is a difference between marker-based and markerless calculation, as described in subsection 3.3.2. The COM of marker-based data is located above the COM marker-less data. There is a slight difference between the data of the high speed cameras and GoPro<sup>®</sup> data (cf Table 7.2). The COM of the GoPro<sup>®</sup> data is in average 5cm below the marker based, compared to 8cm of the high speed cameras. Figure 7.2 shows the COM during the volleyball stroke and a 3D stick diagram with the different COM data. Light blue circles represent the marker based data, the dark blue ones the markerless data of eight cameras and the dark red ones the markerless data of four cameras. Green circles illustrate the GoPro<sup>®</sup> data.

		<b>Body center of mass</b>	
Joint	Camera no	correlation	mean value
COM	8	0.997	0.084
	4	0.999	0.082
	GoPro <sup>®</sup>	0.997	0.053

**Table 7.2:** correlation coefficient & mean value of the body center of mass

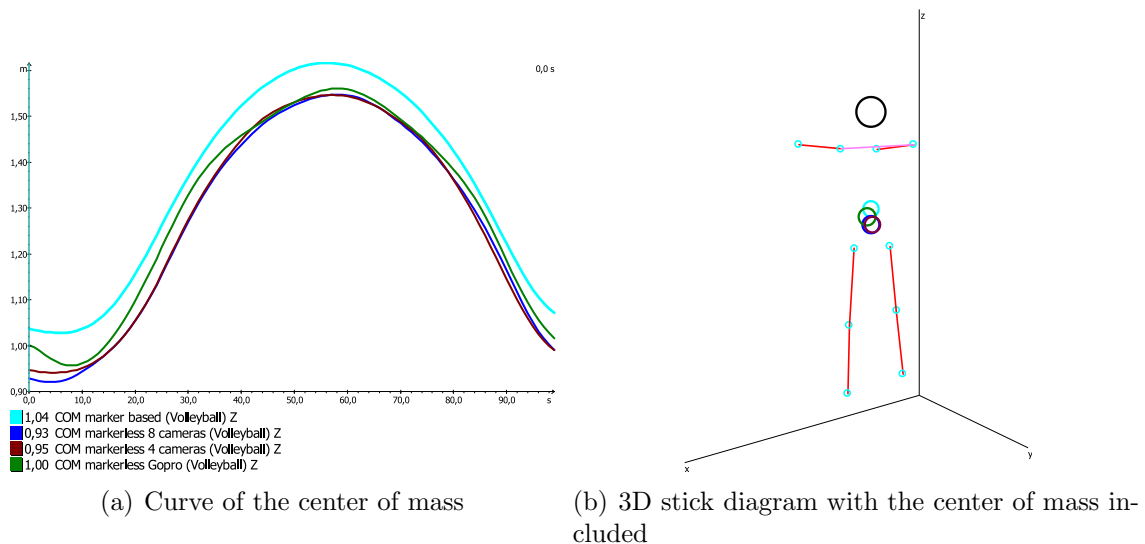


**Figure 7.2:** Location of the center of gravity marker based (light blue) vs. markerless 8 cameras (dark blue); markerless 4 cameras (red) and markerless GoPro<sup>®</sup> (green)

### 7.1.3 Segment velocity and acceleration

The segment velocity and acceleration can be calculated from the segment COM. When comparing all segment velocity data, it is noticeable that the data of the GoPro<sup>®</sup> are worse than those of the markerless high speed data (cf. Table A.17). As expected, due to the mathematical relation between velocity and acceleration, data of the acceleration are even worse. A correlation is no longer available at the GoPro<sup>®</sup> data. Even with high-speed cameras, the correlation drops significantly, but is still in an average range, according to the classification made in Table 2.2. The segment **torso** was chosen as an example because it is the largest segment and tracking in this segment works best. Due to tracking problems in the arms poorer correlations are expected. Figure 7.3 shows the segment velocity and acceleration of the torso in comparison.

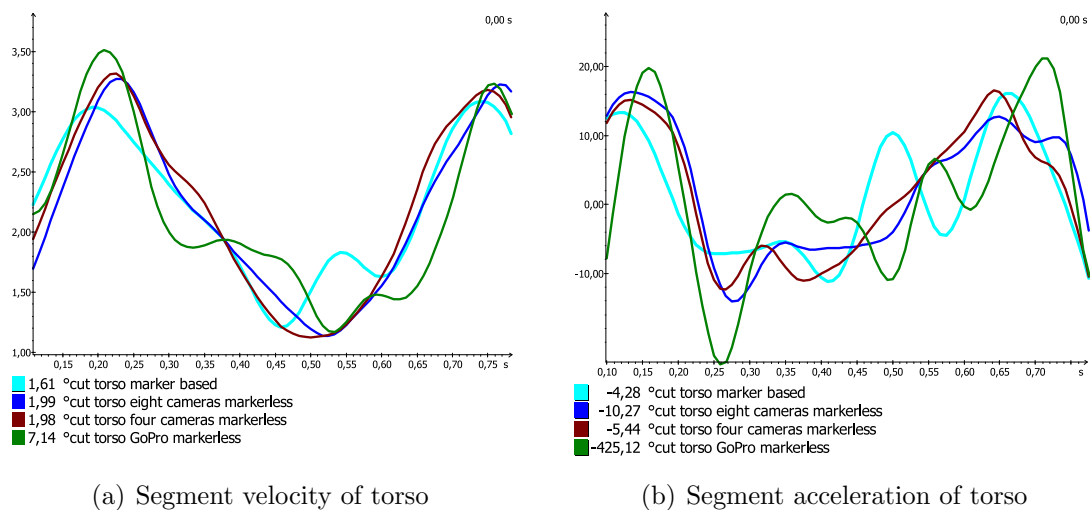


**Figure 7.3:** Comparing velocity and acceleration of the torso  
 light blue: marker, dark blue: eight cameras, red: four cameras, green:  
 GoPro<sup>®</sup> cameras

## 7.2 Handball

### 7.2.1 Joint center

Most of the correlation values are good. In the left ankle there are worse correlations for tracking with eight high speed cameras and tracking with the GoPro<sup>®</sup> cameras. The reason for this is the shadow on the ground and therefore bad segmentation results. When tracking with four cameras the fault of bad segmentation is reduced. The remaining four cameras can be better segmented. Figure 7.4 shows an overview of all positions of the joint centers. The joint centers of the right elbow are the same for all markerless setups, but for the marker based tracking the elbow joint is different. Figure 7.4 (b) shows the curve of the right elbow in the x direction. It is obvious that there is no constant offset, but the data varies enormously. This is why the standard deviation of the mean difference is so high (cf. Table A.14).

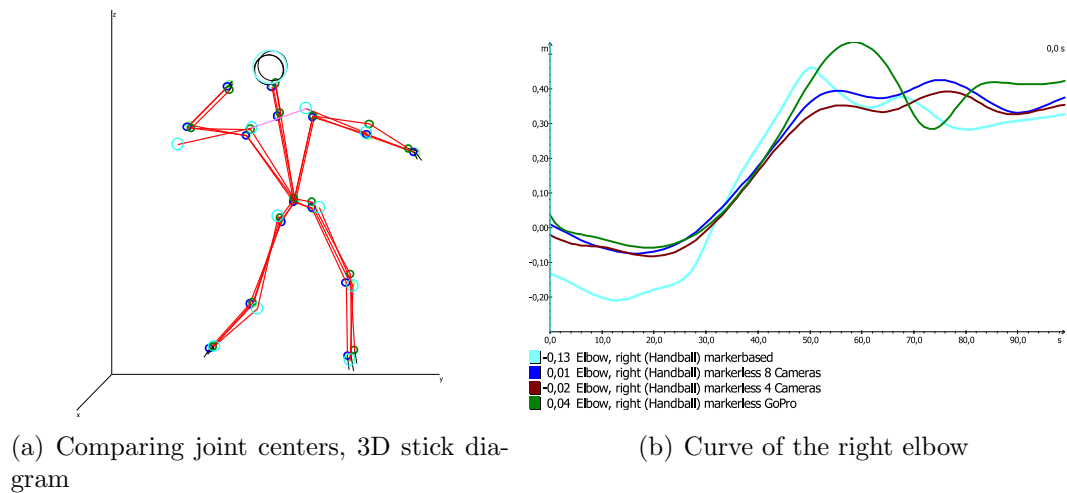


**Figure 7.4:** Comparing the position of joint centers and an exemplary data curve

### 7.2.2 Body center of mass (COM)

Only the data of tracking with eight cameras produce correlations above  $r_s = 0.9$ . Due to a small oscillation at the beginning of the four camera data, the data are consistent with a value of  $r_s = 0.787$  (cf. Figure 7.5 (a)). The data of the GoPro<sup>®</sup> cameras achieve a correlation value of  $r_s = 0.854$ . The standard deviation of the mean deviation is very low ( $\sigma = 0.01$ ) for all setups. This indicates that the values have a low scatter and therefore a constant offset is available. In Table 7.3 the average mean value of the difference is represented. It can be seen that the high speed cameras have a larger deviation as it was also observed in the previous experiment.

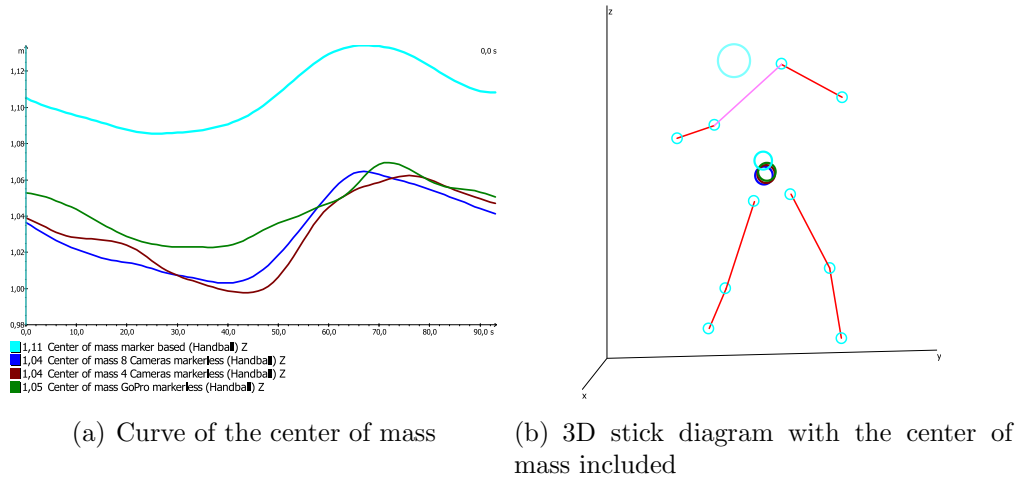


**Figure 7.5:** Location of the center of gravity marker based (light blue) vs. markerless 8 cameras (dark blue); markerless 4 cameras (red) and markerless GoPro<sup>®</sup> (green)

Joint	Camera no	Body center of mass	
		correlation	mean deviation
COM	8	0.913	0.083
	4	0.787	0.084
	GoPro <sup>®</sup>	0.854	0.062

**Table 7.3:** correlation coefficient & mean deviation of the body center of mass

### 7.2.3 Segment velocity and acceleration

As in the previous trials the data of the segment velocity are well again. However, it can be seen that the data of the GoPro<sup>®</sup> cameras has a lower correlation in most of the cases (cf Table A.18). The highest amplitude in the velocity is at the time of haul off. The data of the GoPro<sup>®</sup> does not reach such high values. In addition, the maximum is reached sooner. The second peak of the GoPro<sup>®</sup> data reached a similar height as the first. Whereas the data of the high speed cameras are significantly lower than the first maximum. It is also good to see that there is no difference in the course of the curves between eight and four cameras. The results of the acceleration are very bad in this trial and a correlation is no longer existent, except some segments such as the lower arm as it can be seen in Figure 7.6.

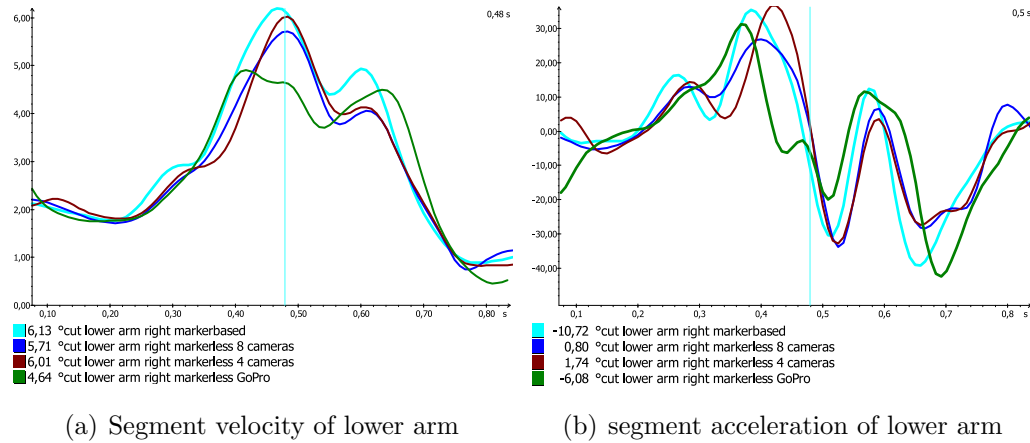


**Figure 7.6:** Comparing velocity and acceleration of the lower arm  
 light blue: marker, dark blue: eight cameras, red: four cameras, green: GoPro<sup>®</sup> cameras

## 7.3 Basketball

Due to the relatively slow movement (cf. section 6.1), there are no problems while tracking.

### 7.3.1 Joint center

All correlation values are above  $r_s = 0.9$  (cf Table A.15). There are no significant differences between the three camera setups. Figure 7.7 shows a 3D stick diagram of the throw. The left knee of the GoPro<sup>®</sup> Data (green circle) is slightly shifted. This results in a similarly shifted hip, and is reflected in the average difference again.

Position of Joint centers			
Joint	Camera no	mean deviation (l/r)	SD of mean value(l/r)
knee	8	0.02 / 0.02	0.02 / 0.01
	4	0.00 / 0.00	0.03 / 0.01
	GoPro <sup>®</sup>	0.01 / 0.02	0.04 / 0.03

**Table 7.4:** Extract from: Table A.15 correlation coefficient & SD of mean value from the joint centers of the knee

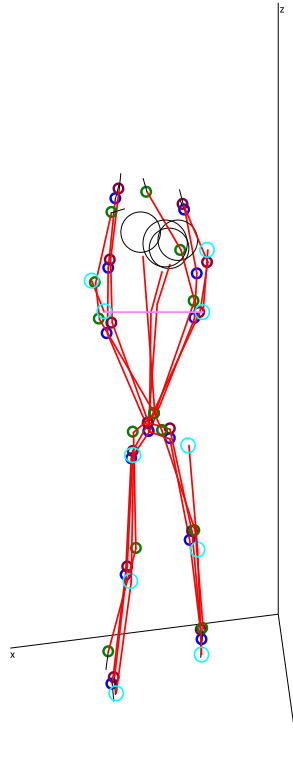


**Figure 7.7:** 3D Stick diagram: marker based joint centers (light blue) vs. markerless 8 cameras (dark blue); markerless 4 cameras (dark red) and markerless GoPro<sup>®</sup> (dark green)

### 7.3.2 Body center of mass (COM)

In contrast to the other movements, this time a different course of the data is observed. At the highest point of the body COM, the curves of the marker based data and the GoPro<sup>®</sup> data are on the same level as it can be seen in Figure 7.8. In the other experiments, a more or less constant offset is adhered. The reason for that could be a highly slipped model when tracking the GoPro<sup>®</sup> data. Figure 7.9 shows an image section of the tracking process. The model overlay is significantly higher than the silhouette during the jump. Although the same model has been used in all trackings, the shifted model can only be observed in the GoPro<sup>®</sup> data. This is due to the rather poor segmentation. In the segmented image it can be seen that the head is no longer visible, furthermore the shoes are only half visible. Figure 7.9 (c) shows a view where the area above the head is not segmented. The software would adjust the head in this area and therefore the model moves up.



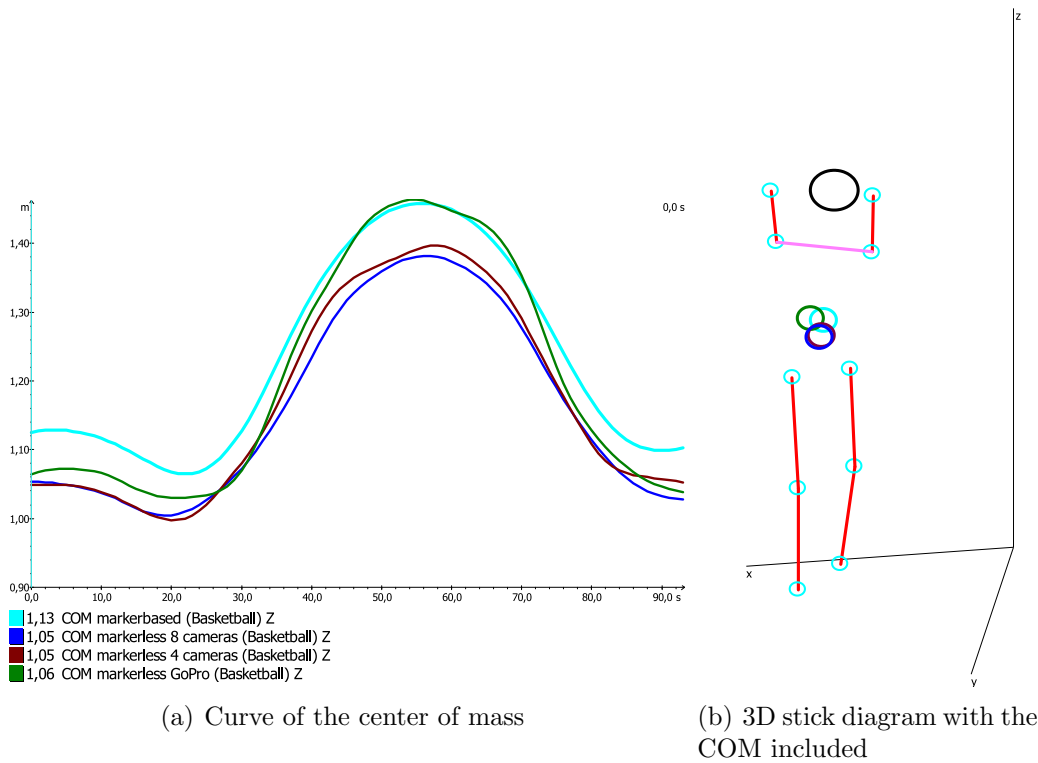


**Figure 7.8:** Location of the center of gravity marker based (light blue) vs. markerless 8 cameras (dark blue); markerless 4 cameras (dark red) and markerless GoPro<sup>®</sup> (dark green)

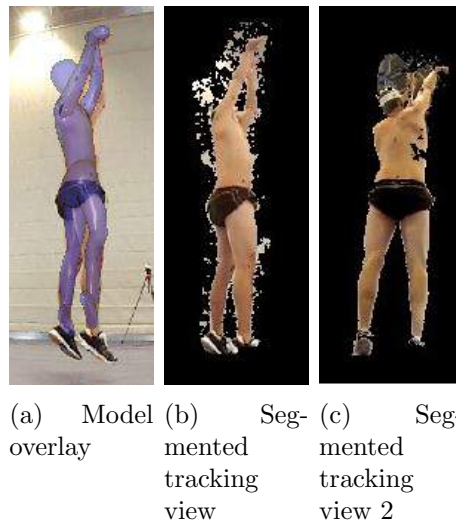


**Figure 7.9:** Image section of the tracking process

### 7.3.3 Segment velocity and acceleration

The results of the segment velocity and acceleration are exactly as they should be. All results for the segment velocity are good for each segment (cf. Table A.19). There is no significant difference between the high speed system and the GoPro<sup>®</sup> system. Looking at the segment acceleration a difference can be observed. Due

to the mathematical relationship between velocity and acceleration, the correlation coefficients are worse. But the data of the high speed cameras are still good, which corresponds to a value above  $r_s = 0.8$ . Merely the data of the GoPro<sup>®</sup> cameras have an average correlation. This was expected, since the correlation values of the velocity were a little worse. Figure 7.10 shows the segment velocity and acceleration of the left lower leg. It can be clearly seen that the GoPro<sup>®</sup> data reproduces much larger amplitudes.

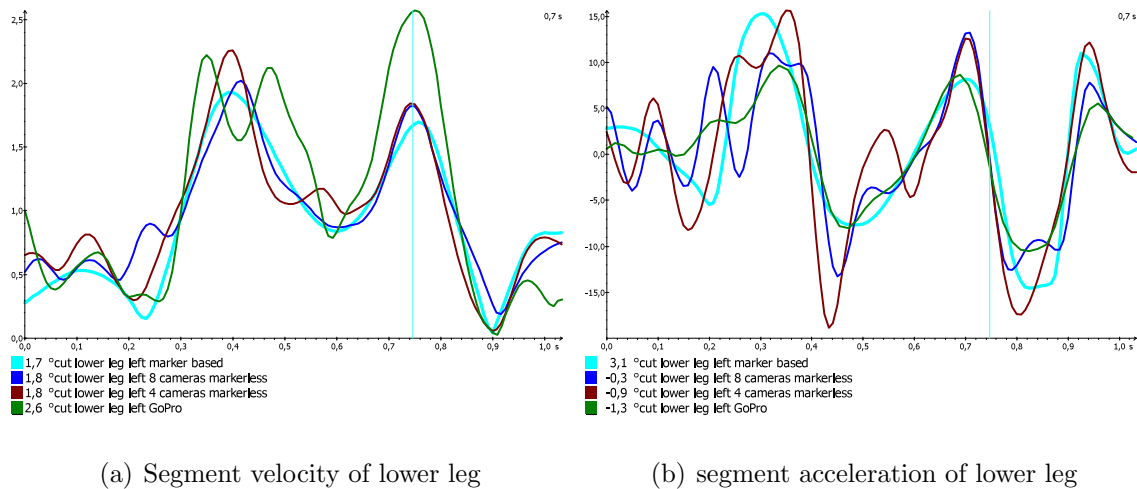


**Figure 7.10:** Comparing velocity and acceleration of the lower leg  
 light blue: marker, dark blue: eight cameras, red: four cameras,  
 green: GoPro<sup>®</sup> cameras

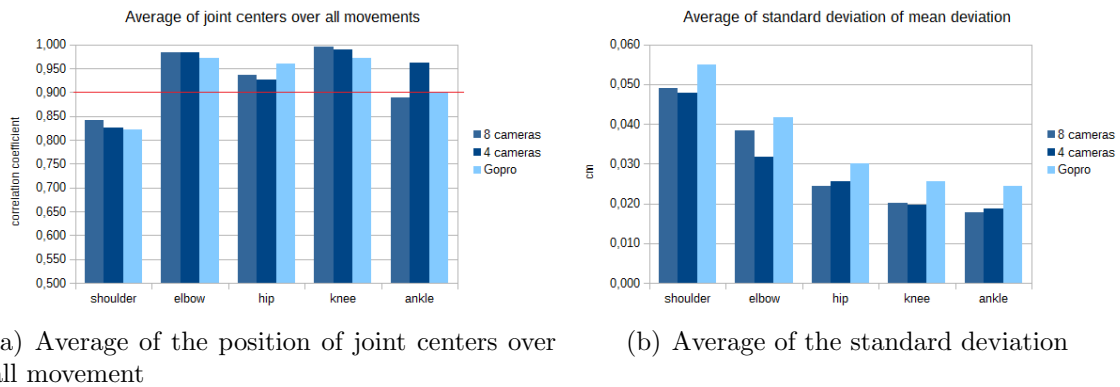
## 7.4 Total Result

### 7.4.1 Joint center

Figure 7.11 shows a bar chart of the average of each joint center across all movements. The red line on the level of  $r_s = 0.9$  illustrates for which joint very good correlation coefficients can be achieved. For most joint centers very good correlations with a value above  $r_s = 0.9$  are achieved. The correlation coefficient of the shoulder joint center achieved the lowest value due to the different defined joint centers and the segmented built model as explained above. It is remarkable that the correlation value of the ankle reaches the highest value for tracking with four cameras. The ankle was hard to track, because the shadow on the ground has led to problems. The segmentation was really bad, because the shadow is also a movement and is counted to the foreground. When tracking with only four cameras, some cameras with bad segmentations do not affect the result. There are still some opportunities in Simi Shape to resolve this issue. For example, the *graph cut* is a feature that

could potentially be used to segment the shadow on the ground. There were no extra features like these tested as the easiest setup was investigated in order to demonstrate that passable results can be achieved even without much effort.

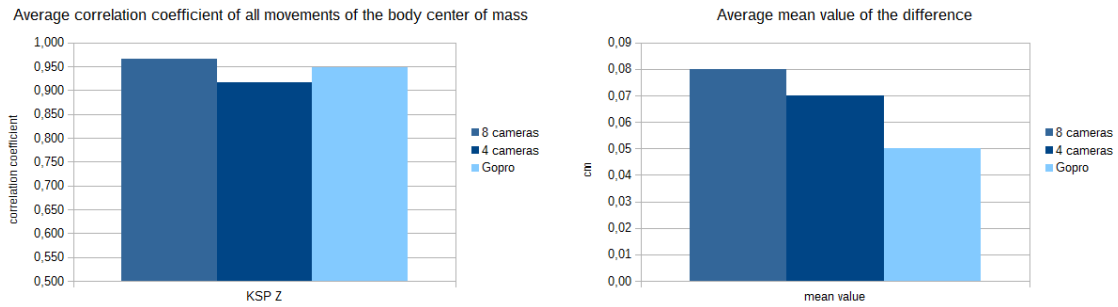
Figure 7.11 (b) shows a bar chart of the average standard deviation of the mean difference of joint centers. The distance between the markerbased and markerless joint centers of the shoulder is greatest. It should be noted that the joint centers of the GoPro<sup>®</sup> data have the highest standard deviation.



**Figure 7.11:** Effect on the accuracy of the position of joint centers and standard deviation of position difference when tracking with low quality cameras

## 7.4.2 Body center of mass (COM)

All average values of the correlation coefficient are above  $r_s = 0.9$ . The correlation coefficient of the GoPro<sup>®</sup> data achieves better values than the data of the markerless tracking with four cameras. Figure 7.12 shows two bar charts: (a) shows the average of the correlation coefficient and (b) the average of mean value of the difference. GoPro<sup>®</sup> data of the average mean value of the difference are closest at the marker data. This is due to the very good but adulterated results of the basketball throw. An adulterated good result can affect the average enormously.



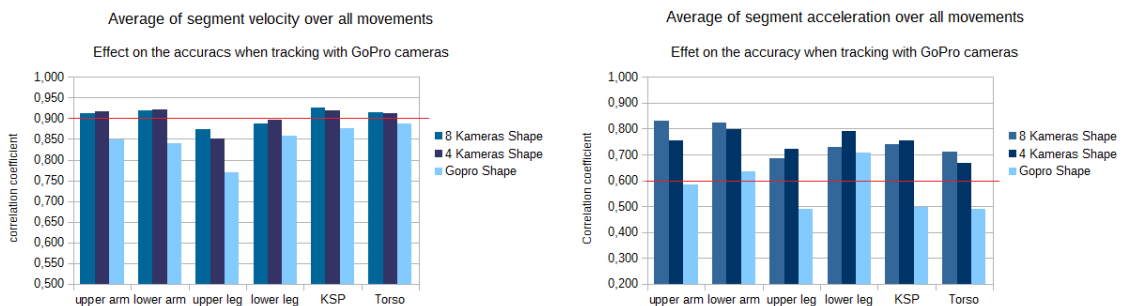
(a) Average of the correlation coefficient of the body center of mass (b) Average of mean value of the difference

Figure 7.12

### 7.4.3 Segment velocity and acceleration

The average for the velocity of all movements and right/left is above  $r_s = 0.8$  (cf Table A.20). This is mainly due to very good correlation values of the basketball throw. Figure 7.13 (a) shows the average of segment velocity across all movements presented in a bar chart. The red line on the level of  $r_s = 0.9$  illustrates which setup achieved very good results. The correlation values for the legs are below this limit at each setup. The data of the high speed cameras always reach a value above  $r_s = 0.9$ . The difference between the two high speed camera setups is extremely slight. The values of the GoPro<sup>®</sup> cameras are always worse. Thus the difference between high speed cameras and action cameras is obvious.

Because of the mathematical relation between velocity and acceleration and the related lower correlation, the limit is set to  $r_s = 0.6$  representing an average correlation. Most of the values of the high speed data are also in this area (cf. Figure 7.13 (b)). The correlation coefficient of the GoPro<sup>®</sup> cameras are even above. Four out of six values are below this limit and thus a very low correlation is available.



(a) Average of segment velocity over all movements (b) Average of segment acceleration over all movements

Figure 7.13: Effect on the accuracy of segment velocity and acceleration when tracking with low quality cameras

## 8 Summary

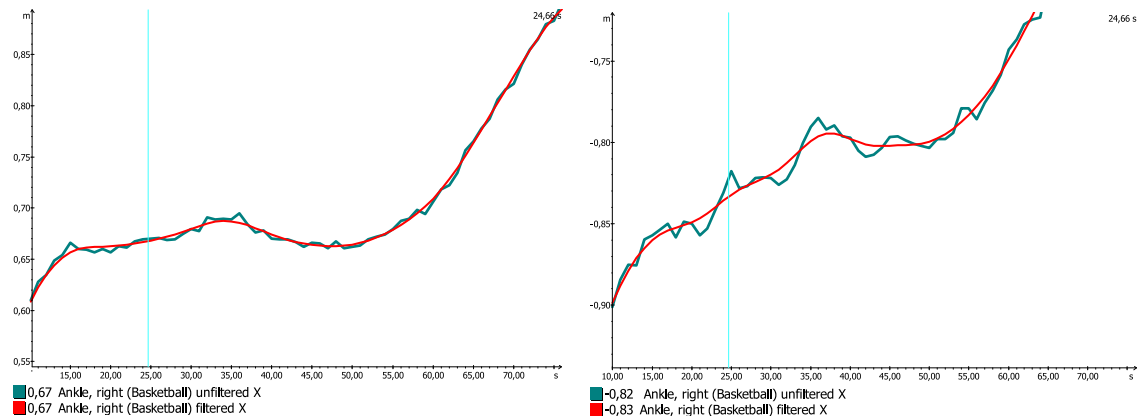
In the following chapter the above-mentioned results are summarized. Problems which have arisen during the process of markerless tracking with action cameras are discussed. It should be emphasized that no hybrid setups were tested in this study. For example, the arm could be performed more stable and improves the results. Therefore no markers are needed necessarily, the arm can be clicked purely visual. As a new setting of Simi Shape, the effect on the accuracy of the function *iterations per frame* has been tested. By increasing this value, the results of the GoPro<sup>®</sup> cameras improve greatly.

Despite the very fast movement of the handball throw there were no problems when tracking with GoPro<sup>®</sup> cameras in contrast to the tracking of the volleyball throw. One possible reason for this is that the fast part of the movement was carried out in the y direction. The resolution of the GoPro<sup>®</sup> cameras in that direction is 1280px in contrast to 720px in the z axis. The pixel offset is only about 3%, ie. 1% less. Furthermore the silhouette of the arm is clearly separated from the body, with the result that a good segmentation is possible. Body parts that are in front of the body are very hard to track, because the software Simi shape can not differentiate. Especially the arms can be a problem. When the arms are in front of the body, the silhouette is difficult to distinguish. As soon as a silhouette is clearly visible again, the tracking can work properly.

Another problem which arises is the segmental built model - which is a general issue with markerless tracking and has nothing to do with the GoPro<sup>®</sup> in particular. Thus no shoulder girdle and spine exist, the mobility is limited in the torso. For example it is not possible to make a hump or an 180° abduction. The tracking of athletic movements is thus limited by the model. The problem is noticeable only in the position of the shoulder joint centers. This problem will be fixed soon, a new model with multiple joints is already in development.

As seen in Figure 7.11 (b) the mean standard deviation of the mean position deviation of joint centers at GoPro<sup>®</sup> data is highest. The meaning of this is that the scatter is relatively large and the values vary greatly. This is because the videos are recorded with a lower frame rate, and thus there is a considerable change from one frame to the next. The model is always readjusted and an orientation on the previous frame is more difficult. This results in larger jumps in the data. By filtering the data variations in the curve occur, which can be prevented by better-quality data. Figure 8.1 shows the comparison between raw and filtered data of high speed and GoPro<sup>®</sup> cameras. It is obvious that there are large steps in the GoPro<sup>®</sup> data which looks jagged. Not only the lower frame rate leads to worse data but also the worse

calibration of GoPro cameras<sup>®</sup>. The standard deviation of the high speed calibration is 1,82mm. In the manual calibration there is not one value for the standard deviation but one for each camera. Two cameras have a good standard deviation and at two cameras the values are not so good. A very large area of 28m<sup>3</sup> was calibrated with the high speed cameras. With the manual calibration a far smaller area of 2.1m<sup>3</sup> was covered. This is too small, even for a good calibration.



(a) Raw data and filtered data of high speed cameras (b) Raw data and filtered data of GoPro<sup>®</sup> cameras

**Figure 8.1:** Comparison between raw and filtered data of high speed cameras and GoPro<sup>®</sup> cameras

This inferior quality of the data leads to the partly large variations in acceleration. By differentiation a function, information is lost resulting in even worse data. The frame rate is also crucial for the quality of the data and therefore for the accuracy. To illustrate the difference between the accuracy of the data, the frame rate of the basketball throw was resampling from 120Hz to 60Hz. For that every second frame was erased and then interpolated. In the course of the joint centers no difference can be seen between 60Hz and 120Hz. Only when calculating the velocity and acceleration of segments differences are identifiable. Figure 8.2 shows the comparison between the velocity and acceleration calculated with 120Hz and 60Hz. Visually a difference in the velocity can only be seen in the amplitudes level. During acceleration the difference is apparent.

At the calculation of the body center of mass a difference between the methods of calculation exist. As seen multiple times in the results, the joint centers of the upper body, especially the shoulder joint centers, of the marker based data are higher. This leads to a different weighting of the upper body and causes a lower center of mass of the markerless data. Since there is no right or wrong in the calculation of

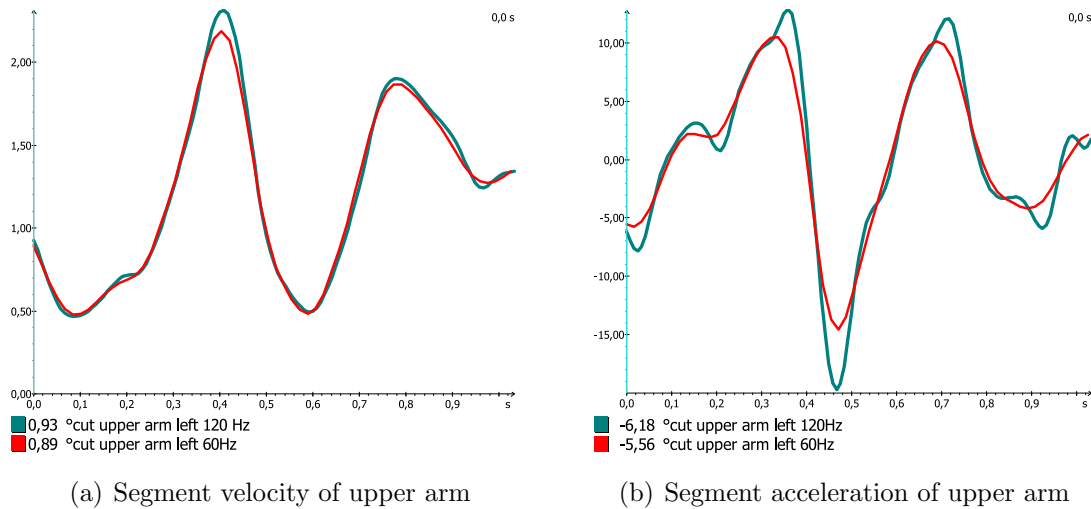


**Figure 8.2:** Comparison between data recorded with 120Hz and recorded with 60Hz

the center of mass and given there are different ways to calculate it, an assessment is difficult. However it is likely that the calculation of the marker based data is closer to reality. Mainly because the Simi Shape model is anatomically not accurate in the shoulder joint.

In conclusion, a slight loss of data quality must be made when recording with GoPro<sup>®</sup> cameras. The joint centers are constantly indicating a good correlation and are uncertain only by the high standard deviation. Even at the segment velocity good correlations can be achieved, only the segment acceleration correlated mediocre. The reasons for the partly worse correlation values can be found mainly in the used GoPro<sup>®</sup> model. Better results can be achieved by using a newer GoPro<sup>®</sup> model. Due to an increased frame rate, higher quality images are expected, which will make tracking easier. The pixel offset would not be as large, which means that the jumps from one frame to the next would be lower. This reduces the jumps in the data curve which significantly affects the quality of the data. Again it should be emphasized that there is no considerable difference between the number of used high speed cameras. It can be concluded that markerless tracking with GoPro<sup>®</sup> cameras is possible. But compromises in accuracy have to be made. It all depends on the question of what should be investigated. Simple pulse sequences and the center of mass position provide good results in comparison with high speed cameras. Joint angle and segment acceleration do not lead to good results. It is also proved that a tracking with four high speed cameras must make no major loss of accuracy. A well chosen camera setup is crucial for good tracking results. Another question for further investigations is whether better GoPro<sup>®</sup> cameras produce better results which can be assumed.

## **Part IV**

**Discussion of the evaluation of  
markerless 3D joint position  
accuracy using high end vs. low  
end camera setups**



# Discussion

As a result of both parts of this work, it is clear that even low end camera setups provide good results. There is hardly any difference when tracking with four instead of eight high speed cameras. If four action cameras used, instead of four expensive high speed cameras, an inferior loss of quality is observed. This is mainly due to the lower frame rate and the non-adjustable shutter speed. In consequence of the lower frame rate, the data must be more interpolated with the result that large jumps occur in the data. Nevertheless, good results can be obtained for some of the examined parameters. For example the position of the body center of mass is good, as long as no tracking problems occurred. The segment velocity and acceleration are difficult to assess when tracking with action cameras. The results of four high speed cameras are closer to the standard of eight cameras and have a higher correlation coefficient.

Which setup is ultimately used depends on the question. The high speed cameras are variable adjustable in frame rate and shutter speed which is a great advantage especially in fast sports movements. The biggest advantage of GoPro<sup>®</sup> cameras is, that they are wireless. This makes them much more variable usable. It should also be noted, that there are also wireless high speed cameras, but they are very expensive and therefore not acceptable for sport science institutes.

In further research the question should be treated whether other GoPro<sup>®</sup> models like the GoPro<sup>®</sup> Hero 4 achieve better results. A good camera setup and a good contrast should always be respected in order to get good results.

# Bibliography

- [1] Basler. *Datenblatt, Basler Scout*. Last accessed on 10/04/2016. URL: <http://www.baslerweb.com/de/produkte/kameras/flaechenkameras/scout/sca640-120gm>.
- [2] Linda Becker. "Evaluation of joint angle accuracy using markerless silhouette-based tracking and hybrid tracking against traditional marker tracking". unveröffentlichte Masterarbeit. MA thesis. Otto-von-Guericke-Universität Magdeburg, Jan. 2016.
- [3] A. L. Bell, D. R. Pedersen, and R. A Brand. "A comparison of the accuracy of several hip center location prediction methods". In: *Journal of Biomechanics* 23 (June 1990), pp. 617–621.
- [4] J. Dal Pupo et al. "Performance and intralimb coordination during a continuous vertical jump test". In: *Brazilian Congress of Biomechanics*. (2013).
- [5] Doccheck. *Schultergelenk*. Last accessed on 10/04/2016. URL: <http://flexikon.doccheck.com/de/Schultergelenk>.
- [6] Fernuni Hagen. *Korrelationskoeffizient*. Last accessed on 15/01/2016. URL: [http://www.fernuni-hagen.de/ksw/neuestatistik/content/MOD\\_23196/html/comp\\_23414.html](http://www.fernuni-hagen.de/ksw/neuestatistik/content/MOD_23196/html/comp_23414.html).
- [7] Simi Realtiy Motion Systems GmbH. *Motion Benutzerhandbuch -Simi Motion version 9.1.1*. Simi Realtiy Motion Systems GmbH. Unterschleißheim, Sept. 2015.
- [8] Simi Realtiy Motion Systems GmbH. *User's Manual Simi Shape Version 2.0.1*. Simi Realtiy Motion Systems GmbH. Unterschleißheim, Apr. 2015.
- [9] GoPro. *Datenblatt, Hero 3 White*. Last accessed on 10/05/2016. URL: [http://cbcdn2.gp-static.com/uploads/product\\_manual/file/63/UM\\_H3White\\_GER\\_REVB\\_WEB.pdf](http://cbcdn2.gp-static.com/uploads/product_manual/file/63/UM_H3White_GER_REVB_WEB.pdf).
- [10] GoPro. *Datenblatt, Hero 4 Silver*. Last accessed on 10/05/2016. URL: [http://cbcdn2.gp-static.com/uploads/product\\_manual/file/491/UM\\_H4Black\\_GER\\_REVA\\_WEB.pdf](http://cbcdn2.gp-static.com/uploads/product_manual/file/491/UM_H4Black_GER_REVA_WEB.pdf).
- [11] B. Jaehne. *Digitale Bildverarbeitung: und Bildgewinnung*. Springer, 2012.
- [12] Jutta Merten. *Bewegungsrichtungen*. Last accessed on 15/01/2016. URL: <http://www.muskelaufbau-forum.de/planer/Bewegungen.jpg>.
- [13] medilearn. *Allgemein, Achsen und Ebenen*. Last accessed on 03/02/2016. URL: <http://www.medi-learn.de/examen/PDFs/Ana5/17e44461da940331c7c870cbee5c32d7.pdf>.

- 
- [14] medistat GmbH. *Rangkorrelationskoeffizient nach Spearman*. Last accessed on 15/01/2016. URL: <https://www.medistat.de/glossar/korrelation-assoziation/rangkorrelationskoeffizient-nach-spearman/>.
- [15] De Leva P. "Joint center longitudinal positions computed from a selected subset of Chandler's data". In: *Journal of Biomechanics* 29 (Sept. 1996), p. 1231.
- [16] J. Richards. *Biomechanics in clinic and research*. Churchill Livingstone, 2008.
- [17] A. Schär. *Statistik: Grundlagen, Beispiele und Anwendungen gelöst mit Excel ; [eine Einführung in die Statistik für Fachhochschulen, Hochschulen und die höhere Berufsbildung]*. Compendio Bildungsmedien AG, 2003.
- [18] webstyle-berlin.de. *Gelenkarten*. Last accessed on 15/01/2016. URL: <http://www.mfb-wissen.de/Rettsan/Bewegu12.JPG>.
- [19] wikipedia. *Anatomische Lage- und Richtungsbezeichnungen*. Last accessed on 08/02/2016. URL: [https://upload.wikimedia.org/wikipedia/commons/thumb/d/d6/Human\\_anatomy\\_Koerperebenen.svg/2000px-Human\\_anatomy\\_Koerperebenen.svg.png](https://upload.wikimedia.org/wikipedia/commons/thumb/d/d6/Human_anatomy_Koerperebenen.svg/2000px-Human_anatomy_Koerperebenen.svg.png).
- [20] J. D. Willson, S. Binder-Macleod, and I. S. Davis. "Lower Extremity Jumping Mechanics of Female Athletes With and Without Patellofemoral Pain Before and After Exertion". In: *American Journal of Sport Medicine* 36 (May 2008), pp. 1587–1569.

# A Appendix

## Tables: Part II

Segment	Camera No.	Segment velocity		Segment acceleration	
		Correlation left	Correlation right	Correlation left	Correlation right
upper arm	8 Cameras	0.979	0.976	0.968	0.962
	6 Cameras	0.969	0.966	0.933	0.929
	4 Cameras	0.949	0.964	0.918	0.939
	3 Cameras	0.923	0.934	0.872	0.897
lower arm	8 Cameras	0.971	0.967	0.945	0.951
	6 Cameras	0.973	0.963	0.911	0.927
	4 Cameras	0.937	0.944	0.855	0.911
	3 Cameras	0.893	0.896	0.769	0.841
upper leg	8 Cameras	0.932	0.930	0.901	0.908
	6 Cameras	0.922	0.908	0.855	0.837
	4 Cameras	0.908	0.930	0.867	0.890
	3 Cameras	0.868	0.904	0.804	0.855
lower leg	8 Cameras	0.967	0.975	0.940	0.940
	6 Cameras	0.942	0.957	0.887	0.886
	4 Cameras	0.936	0.964	0.893	0.919
	3 Cameras	0.889	0.954	0.859	0.924

**Table A.1:** Average of segment velocity and acceleration

Segment	Camera No.	Segment velocity		Segment acceleration	
		Correlation	Correlation	Correlation	Correlation
COP	8 Cameras	0.988		0.987	
	6 Cameras	0.982		0.968	
	4 Cameras	0.987		0.980	
	3 Cameras	0.976		0.968	
Head	8 Cameras	0.969		0.957	
	6 Cameras	0.958		0.933	
	4 Cameras	0.964		0.957	
	3 Cameras	0.963		0.944	
Torso	8 Cameras	0.969		0.955	
	6 Cameras	0.960		0.934	
	4 Cameras	0.958		0.937	
	3 Cameras	0.937		0.913	

**Table A.2:** Average of segment velocity and acceleration

Joint	Camera No	Position of joint centers			
		Correlation		Distance [m]	
		left	right	left	right
shoulder	8 Cameras	0.988	0.994	0.07	0.07
	6 Cameras	0.992	0.991	0.07	0.08
	4 Cameras	0.997	0.996	0.07	0.07
	3 Cameras	0.990	0.997	0.07	0.07
elbow	8 Cameras	0.993	0.996	0.04	0.03
	6 Cameras	0.996	0.996	0.04	0.04
	4 Cameras	0.991	0.994	0.04	0.03
	3 Cameras	0.980	0.993	0.03	0.05
hip	8 Cameras	0.964	0.951	0.08	0.06
	6 Cameras	0.960	0.945	0.08	0.07
	4 Cameras	0.970	0.951	0.07	0.06
	3 Cameras	0.941	0.955	0.05	0.07
knee	8 Cameras	0.981	0.967	-0.01	0.01
	6 Cameras	0.984	0.970	-0.01	0.01
	4 Cameras	0.977	0.962	-0.01	0.01
	3 Cameras	0.902	0.944	-0.02	0.01
ankle	8 Cameras	0.970	0.980	0.01	0.02
	6 Cameras	0.942	0.967	0.01	0.01
	4 Cameras	0.963	0.975	0.01	0.02
	3 Cameras	0.963	0.956	0.01	0.02

**Table A.3:** Average Correlation coefficient of the position of the Joint centers and the average distance [m] between markerless and marker based Joint centers

Joint	Camera No.	Flexion/Extension		Abduction/Adduction		Rotation			
		Correlation	SD of angle diff. [°]	Correlation	SD of angle diff. [°]	Correlation	SD of angle diff. [°]		
		left	right	left	right	left	right		
shoulder	8 Cameras	0.90	0.95	0.92	0.91	0.22	-0.22	56.37	61.29
	6 Cameras	0.89	0.96	0.95	0.90	0.51	-0.45	30.80	66.76
	4 Cameras	0.83	0.95	0.84	0.93	0.63	-0.45	25.51	98.32
	3 Cameras	0.81	0.89	0.70	0.95	-0.01	0.34	99.41	42.00
elbow	8 Cameras	0.56	-0.79						
	6 Cameras	0.84	-0.78						
	4 Cameras	0.88	-0.80						
	3 Cameras	0.08	0.22						
hip	8 Cameras	0.97	0.97	0.51	0.33	0.72	0.45	9.56	17.54
	6 Cameras	0.95	0.95	0.19	0.08	0.76	0.48	10.95	18.26
	4 Cameras	0.96	0.96	0.32	-0.10	0.41	0.48	21.28	19.02
	3 Cameras	0.91	0.87	0.17	0.43	-0.45	0.36	18.93	21.95
knee	8 Cameras	0.99	0.98						
	6 Cameras	0.99	0.98						
	4 Cameras	0.96	0.98						
	3 Cameras	0.89	0.98						
ankle	8 Cameras	0.98	0.97	0.49	0.79	0.85	0.375	5.11	17.93
	6 Cameras	0.98	0.98	0.44	0.70	0.815	0.41	5.98	17.63
	4 Cameras	0.96	0.98	0.28	0.68	0.567	0.30	18.29	18.68
	3 Cameras	0.96	0.95	0.61	0.41	0.126	0.40	13.04	16.45

Table A.4: Jump: Both legs

Joint	Camera No.	Flexion/Extension		Abduction/Adduction		Rotation							
		Correlation	SD of angle diff. [°]	Correlation	SD of angle diff. [°]	Correlation	SD of angle diff. [°]						
		left	right	left	right	left	right						
shoulder	8 Cameras	0.91	0.97	10.43	15.21	0.94	0.92	3.65	4.05	0.89	-0.56	7.73	163.64
	6 Cameras	0.89	0.96	11.12	13.89	0.934	0.94	3.34	3.39	0.87	0.85	9.45	14.92
	4 Cameras	0.82	0.97	13.56	13.75	0.940	0.89	3.55	3.48	0.76	-0.62	14.33	160.35
	3 Cameras	0.77	0.93	12.24	15.19	0.958	0.90	3.09	4.24	-0.18	0.75	122.03	18.13
elbow	8 Cameras	0.86	-0.70	6.47	23.59								
	6 Cameras	0.73	0.88	6.89	4.91								
	4 Cameras	0.91	-0.90	6.08	24.52								
	3 Cameras	-0.82	0.92	40.49	5.30								
hip	8 Cameras	0.97	0.98	3.54	4.29	-0.180	0.73	5.27	4.54	0.78	0.56	6.48	6.37
	6 Cameras	0.96	0.98	4.51	5.99	-0.16	0.74	5.51	4.67	0.75	0.61	6.38	7.33
	4 Cameras	0.96	0.97	6.16	7.01	-0.38	0.72	6.18	5.34	0.78	0.47	6.44	6.77
	3 Cameras	0.93	0.95	7.13	6.22	-0.34	0.56	6.68	6.91	0.87	0.73	5.71	8.88
knee	8 Cameras	0.95	0.98	2.39	2.73								
	6 Cameras	0.95	0.98	2.39	2.45								
	4 Cameras	0.95	0.97	2.35	3.05								
	3 Cameras	0.93	0.97	2.59	2.98								
ankle	8 Cameras	0.72	0.90	3.95	4.74	-0.28	-0.64	6.34	6.13	-0.34	0.77	5.52	5.23
	6 Cameras	0.68	0.91	5.12	6.19	-0.06	-0.56	7.02	5.77	-0.34	0.76	6.79	6.71
	4 Cameras	0.70	0.91	6.52	4.86	-0.05	0.11	9.68	4.51	-0.42	0.73	7.59	6.03
	3 Cameras	0.61	0.89	9.03	4.49	-0.08	0.19	8.84	3.52	-0.51	0.77	7.67	8.58

Table A.5: Jump: Right leg

Joint	Camera No.	Flexion/Extension		Abduction/Adduction		Rotation			
		Correlation	SD of angle diff. [°]	Correlation	SD of angle diff. [°]	Correlation	SD of angle diff. [°]		
		left	right	left	right	left	right		
shoulder	8 Cameras	0.96	0.96	0.97	0.98	0.94	-0.59	11.4	157.03
	6 Cameras	0.98	0.97	0.97	0.98	0.96	0.923	9.89	9.30
	4 Cameras	0.98	0.97	0.96	0.98	0.92	-0.583	14.52	161.24
	3 Cameras	0.72	0.94	0.92	0.98	-0.10	0.927	146.04	9.99
elbow	8 Cameras	0.97	-0.94						
	6 Cameras	0.97	0.96						
	4 Cameras	0.97	-0.95						
	3 Cameras	-0.92	0.91						
hip	8 Cameras	0.96	0.95	0.42	0.32	0.48	0.41	9.88	7.42
	6 Cameras	0.97	0.88	0.54	0.41	0.49	0.37	9.03	7.46
	4 Cameras	0.93	0.71	0.22	0.28	0.43	0.28	11.55	7.92
	3 Cameras	0.92	0.39	0.18	0.30	0.27	0.20	11.56	7.91
knee	8 Cameras	0.88	0.97						
	6 Cameras	0.88	0.97						
	4 Cameras	0.87	0.94						
	3 Cameras	0.83	0.90						
ankle	8 Cameras	0.93	0.89	-0.15	0.39	0.56	0.38	7.22	3.12
	6 Cameras	0.93	0.82	-0.16	0.45	0.50	0.20	7.50	3.27
	4 Cameras	0.90	0.72	-0.31	0.20	0.50	0.20	7.69	3.19
	3 Cameras	0.92	0.68	-0.08	0.21	0.40	0.34	7.91	3.11

Table A.6: Jump: Left leg



Joint	Camera No.	Flexion/Extension		Abduction/Adduction		Rotation							
		Correlation	SD of angle diff. [°]	Correlation	SD of angle diff. [°]	Correlation	SD of angle diff. [°]						
		left	right	left	right	left	right						
shoulder	8 Cameras	0.90	0.94	16.93	31.11	0.96	0.83	4.72	7.05	0.89	0.48	17.28	52.74
	6 Cameras	0.90	0.97	16.91	12.22	0.96	0.84	4.66	7.05	0.88	0.57	17.45	46.17
	4 Cameras	0.91	0.93	17.29	14.76	0.96	0.80	5.82	7.61	0.81	0.85	23.09	17.12
	3 Cameras	0.80	0.81	20.48	27.24	0.92	0.69	7.62	11.30	0.71	0.33	25.67	81.39
elbow	8 Cameras	0.74	0.46	9.431	73.28								
	6 Cameras	0.76	0.77	8.69	55.90								
	4 Cameras	0.74	0.89	12.10	11.60								
	3 Cameras	0.78	0.45	11.55	85.93								
hip	8 Cameras	0.88	0.92	7.79	7.59	0.68	0.56	8.04	8.81	0.64	0.44	11.65	9.12
	6 Cameras	0.84	0.91	8.28	8.15	0.66	0.56	7.94	8.36	0.61	0.33	11.66	9.99
	4 Cameras	0.77	0.89	11.64	10.15	0.73	0.65	7.00	6.73	0.48	0.14	12.10	13.47
	3 Cameras	0.67	0.76	13.07	13.33	0.47	0.47	10.18	9.75	0.26	0.14	15.36	19.18
knee	8 Cameras	0.97	0.96	2.45	2.40								
	6 Cameras	0.97	0.96	2.36	2.06								
	4 Cameras	0.97	0.97	2.23	2.20								
	3 Cameras	0.93	0.94	3.17	3.56								
ankle	8 Cameras	0.94	0.90	3.43	4.34	0.48	0.59	5.33	4.85	0.37	0.35	8.98	9.00
	6 Cameras	0.91	0.88	3.45	4.66	0.49	0.56	5.41	5.11	0.36	0.28	8.88	10.01
	4 Cameras	0.85	0.87	5.67	5.05	0.25	0.43	7.20	6.00	0.42	0.23	8.58	11.18
	3 Cameras	0.81	0.84	5.81	6.27	0.29	0.07	6.96	8.08	0.35	0.10	8.33	12.55

Table A.7: Kick and Box

Joint	Camera No.	Flexion/Extension		Abduction/Adduction		Rotation							
		Correlation	SD of angle diff. [°]	Correlation	SD of angle diff. [°]	Correlation	SD of angle diff. [°]						
		left	right	left	right	left	right						
shoulder	8 Cameras	-0.49	0.84	2.41	7.79	0.92	0.70	0.86	1.02	0.10	-0.57	4.25	8.91
	6 Cameras	0.35	0.98	1.89	0.73	0.91	0.40	0.55	1.02	0.35	-0.17	4.10	10.49
	4 Cameras	-0.72	0.94	1.45	1.17	-0.77	-0.06	3.87	1.34	-0.72	0.56	31.49	4.63
	3 Cameras	0.46	0.80	1.77	1.93	0.82	-0.38	1.04	2.17	0.46	0.09	5.71	29.20
elbow	8 Cameras	0.70	0.39	2.11	4.80								
	6 Cameras	0.66	0.65	1.27	1.64								
	4 Cameras	0.62	-0.78	2.74	4.28								
	3 Cameras	0.72	0.43	1.12	2.79								
hip	8 Cameras	0.89	0.97	4.28	5.01	-0.46	-0.36	4.99	5.92	-0.77	-0.71	5.11	7.56
	6 Cameras	0.89	0.98	4.60	5.25	-0.15	-0.40	5.17	6.56	-0.60	-0.77	6.10	8.80
	4 Cameras	0.95	0.96	3.57	3.64	0.13	0.08	4.14	5.25	-0.49	-0.65	4.64	6.06
	3 Cameras	0.98	0.84	3.65	7.36	0.25	0.11	5.15	6.64	-0.24	-0.64	8.20	12.65
knee	8 Cameras	0.99	0.99	1.24	2.78								
	6 Cameras	0.99	0.99	1.18	2.49								
	4 Cameras	0.99	0.99	2.83	1.48								
	3 Cameras	0.97	0.99	2.55	2.36								
ankle	8 Cameras	0.63	0.95	7.92	5.18	0.05	-0.68	3.78	4.96	-0.53	0.76	7.14	3.14
	6 Cameras	0.79	0.96	8.13	4.90	-0.07	-0.80	3.90	9.39	-0.35	0.72	5.83	4.56
	4 Cameras	0.67	0.94	7.51	3.60	0.26	-0.81	9.31	9.82	0.32	0.56	8.26	7.56
	3 Cameras	0.07	0.83	14.27	10.04	0.00	-0.69	9.44	10.13	-0.66	0.49	13.95	8.95

Table A.8: Biking

Joint	Camera No.	Flexion/Extension		Abduction/Adduction		Rotation	
		Correlation	SD of angle diff. [°]	Correlation	SD of angle diff. [°]	Correlation	SD of angle diff. [°]
		left	right	left	right	left	right
hip	8 Cameras	0.47	0.52	0.94	0.91	0.11	0.70
	6 Cameras	0.40	0.56	0.95	0.92	0.15	0.78
	4 Cameras	0.44	0.31	0.92	0.88	-0.24	0.65
	3 Cameras	0.60	0.78	0.94	0.88	0.03	0.84
knee	8 Cameras	0.96	0.99				
	6 Cameras	0.99	0.96				
	4 Cameras	0.95	0.95				
	3 Cameras	0.98	0.92				
ankle	8 Cameras	0.92	0.95	0.21	0.28	0.48	0.32
	6 Cameras	0.92	0.97	0.03	0.25	0.52	0.05
	4 Cameras	0.93	0.93	-0.01	0.36	0.44	0.21
	3 Cameras	0.91	0.97	-0.10	0.16	-0.35	0.46

Table A.9: Jumping Jack

Joint	Camera No.	Flexion/Extension		Abduction/Adduction		Rotation			
		Correlation	SD of angle diff. [°]	Correlation	SD of angle diff. [°]	Correlation	SD of angle diff. [°]		
		left	right	left	right	left	right		
shoulder	8 Cameras	0.98	0.97	0.82	0.92	0.30	0.17	8.96	5.13
	6 Cameras	0.95	0.97	0.80	0.93	0.36	0.63	5.22	4.07
	4 Cameras	0.87	0.88	0.82	0.93	-0.10	0.01	13.55	6.11
	3 Cameras	0.86	0.91	0.70	0.89	-0.73	0.47	15.92	10.61
elbow	8 Cameras	-0.74	0.91						
	6 Cameras	0.68	0.70						
	4 Cameras	0.71	0.83						
	3 Cameras	0.48	0.89						
hip	8 Cameras	0.75	0.96	0.34	0.21	-0.01	-0.18	9.91	11.41
	6 Cameras	0.89	0.93	0.25	0.37	-0.12	-0.08	13.95	14.94
	4 Cameras	0.77	0.95	0.56	0.30	0.24	-0.24	7.58	8.78
	3 Cameras	0.51	0.96	0.29	0.31	-0.06	-0.28	8.46	7.73
knee	8 Cameras	0.98	0.99						
	6 Cameras	0.97	0.96						
	4 Cameras	0.98	0.99						
	3 Cameras	0.99	0.99						
ankle	8 Cameras	0.96	0.95	0.02	0.37	0.43	0.49	7.09	9.01
	6 Cameras	0.84	0.98	-0.26	0.47	0.41	0.48	8.98	11.10
	4 Cameras	0.79	0.91	-0.36	0.17	0.38	0.59	7.47	6.38
	3 Cameras	0.97	0.97	-0.27	0.04	0.34	0.61	8.03	5.60

Table A.10: Running: Small steps

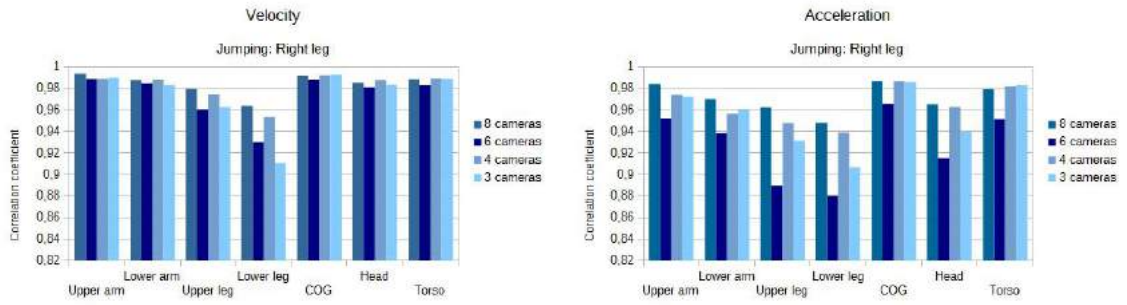
Joint	Camera No.	Flexion/Extension		Abduction/Adduction		Rotation							
		Correlation	SD of angle diff. [°]	Correlation	SD of angle diff. [°]	Correlation	SD of angle diff. [°]						
		left	right	left	right	left	right						
shoulder	8 Cameras	0.92	0.97	3.44	3.04	0.71	0.97	1.28	2.05	0	0.78	72.33	4.39
	6 Cameras	0.95	0.95	2.82	5.40	0.48	0.94	2.02	2.99	0.42	0.88	4.74	5.38
	4 Cameras	0.78	0.92	5.14	6.52	0.54	0.94	2.63	2.88	-0.39	0.77	13.72	5.23
	3 Cameras	0.78	0.94	5.01	11.13	0.09	0.96	4.84	2.28	-0.10	0.80	11.77	12.73
elbow	8 Cameras	-0.73	0.97	7.55	1.70								
	6 Cameras	0.66	0.94	4.07	2.21								
	4 Cameras	0.61	0.95	2.90	2.61								
	3 Cameras	0.38	0.69	4.49	5.64								
hip	8 Cameras	0.94	0.96	7.35	5.85	0.68	0.02	2.31	3.42	0.28	-0.19	11.80	12.53
	6 Cameras	0.97	0.96	5.32	3.22	0.33	-0.13	3.05	3.67	0.16	-0.30	15.99	17.38
	4 Cameras	0.72	0.90	10.65	10.12	0.63	-0.12	2.64	4.70	0.65	-0.02	7.51	9.73
	3 Cameras	0.44	0.93	13.63	14.16	0.39	-0.16	6.18	6.90	0.29	0.02	11.04	10.90
knee	8 Cameras	0.99	0.99	1.20	1.18								
	6 Cameras	0.99	0.99	1.83	2.57								
	4 Cameras	0.99	0.99	1.41	1.32								
	3 Cameras	0.99	0.99	3.03	2.18								
ankle	8 Cameras	0.97	0.99	3.24	1.86	-0.03	0.34	5.68	3.54	0.25	0.24	10.31	10.57
	6 Cameras	0.97	0.98	3.27	2.22	-0.42	-0.10	5.44	5.13	0.10	0.22	11.00	11.22
	4 Cameras	0.93	0.97	4.95	3.07	-0.28	-0.29	4.79	5.65	0.12	0.46	11.53	7.29
	3 Cameras	0.94	0.98	5.21	2.17	-0.19	-0.39	5.90	4.90	0.24	0.50	9.57	7.02

Table A.11: Running: Large steps

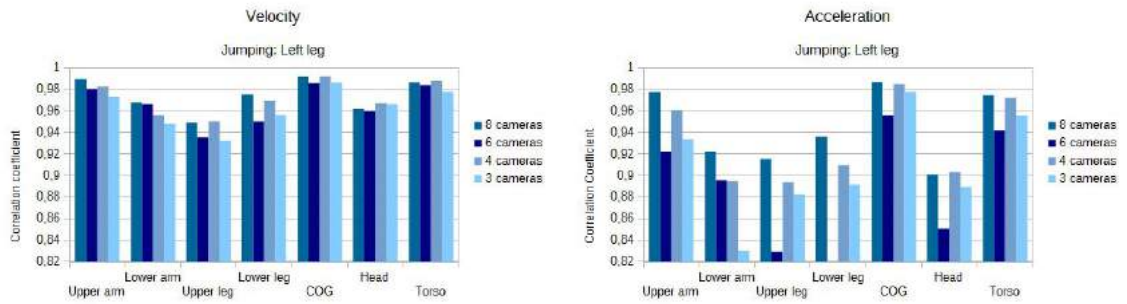
Joint	Camera No.	Flexion/Extension		Abduction/Adduction		Rotation	
		Correlation	SD of angle diff. [°]	Correlation	SD of angle diff. [°]	Correlation	SD of angle diff. [°]
shoulder	8 Cameras	0.950	9.82	0.905	3.26	0.275	51.525
	6 Cameras	0.950	7.24	0.855	2.83	0.543	17.053
	4 Cameras	0.906	8.35	0.695	3.49	0.175	42.086
	3 Cameras	0.851	12.16	0.723	4.17	0.269	45.042
elbow	8 Cameras	0.165	20.32				
	6 Cameras	0.677	11.19				
	4 Cameras	0.337	12.07				
	3 Cameras	0.374	20.85				
hip	8 Cameras	0.883	6.25	0.355	4.51	0.235	9.535
	6 Cameras	0.881	6.43	0.324	4.49	0.228	10.906
	4 Cameras	0.828	8.42	0.380	4.69	0.211	10.289
	3 Cameras	0.782	13.08	0.330	6.93	0.148	11.640
knee	8 Cameras	0.977	2.35				
	6 Cameras	0.975	2.33				
	4 Cameras	0.969	2.89				
	3 Cameras	0.954	3.30				
ankle	8 Cameras	0.913	4.33	0.139	5.28	0.363	7.878
	6 Cameras	0.910	4.69	0.060	5.67	0.324	8.558
	4 Cameras	0.878	4.91	0.040	6.35	0.353	9.169
	3 Cameras	0.836	6.24	0.023	6.47	0.235	8.894

Table A.12: Average over all movements and right/left

# Diagrams



**Figure A.1:** Correlation coefficient of Velocity and Acceleration of segment COM: Jumping right leg only



**Figure A.2:** Correlation coefficient of Velocity and Acceleration of segment COM: Jumping left leg only

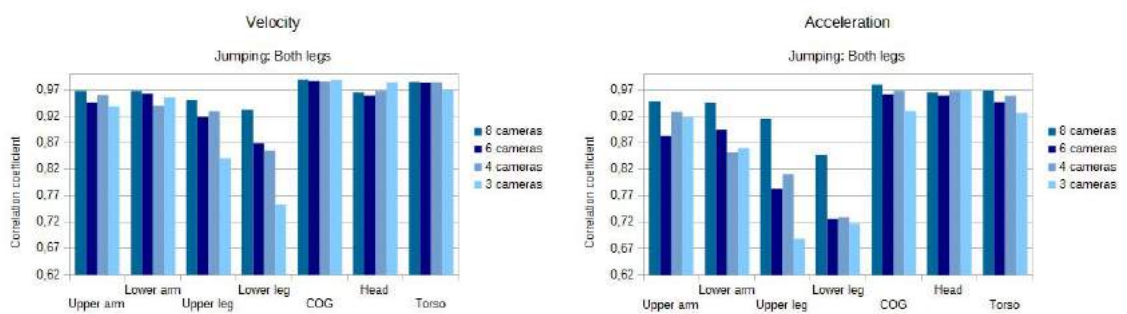


**Figure A.3:** Correlation coefficient of Velocity and Acceleration of segment COM: Jumping both leg

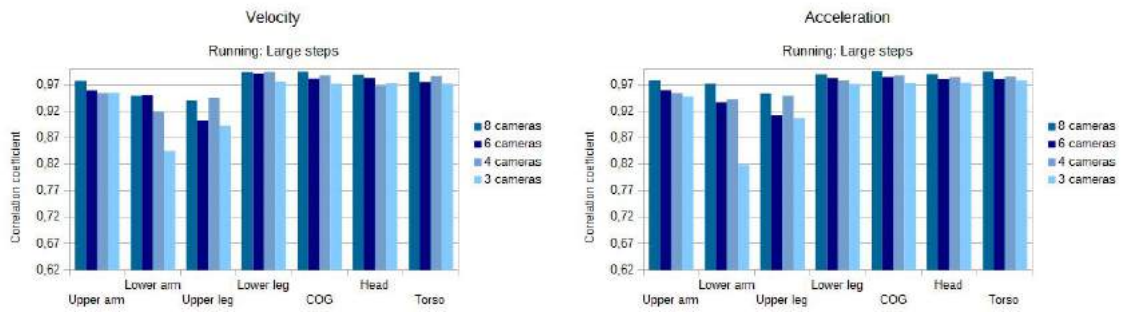


Figure A.4: Correlation coefficient of Velocity and Acceleration of segment COM: Running: large steps

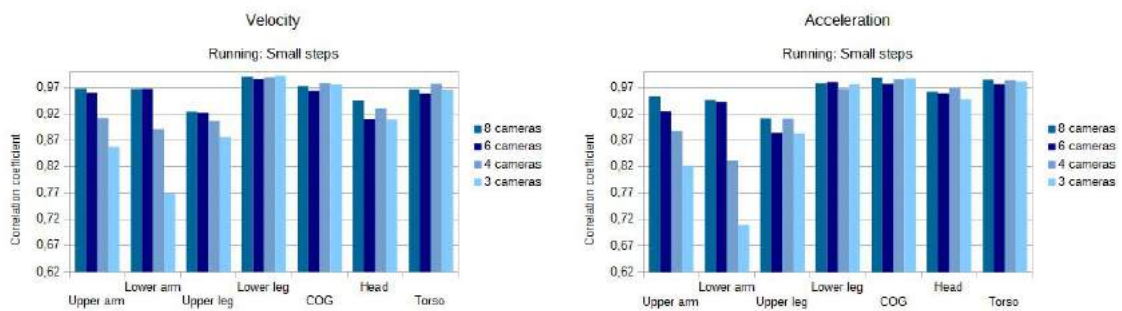


Figure A.5: Correlation coefficient of Velocity and Acceleration of segment COM: Running: small steps

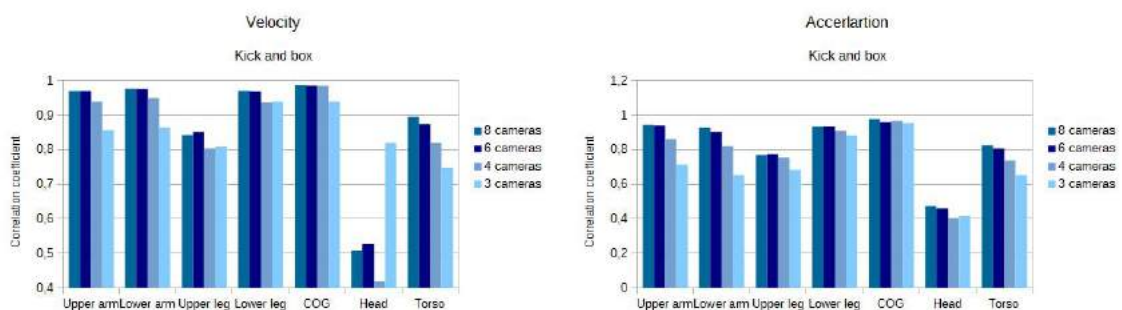


Figure A.6: Correlation coefficient of Velocity and Acceleration of segment COM: Kickbox

### Tables: Part III



Joint	Camera No.	Joint centers			
		correlation		SD	
		left	right	left	right
shoulder	8 cameras	0.994	0.914	0.03	0.05
	4 cameras	0.990	0.914	0.03	0.04
	GoPro <sup>®</sup>	0.992	0.893	0.03	0.06
elbow	8 cameras	0.973	0.996	0.04	0.02
	4 cameras	0.980	0.996	0.04	0.02
	GoPro <sup>®</sup>	0.975	0.984	0.04	0.06
hip	8 cameras	0.918	0.898	0.03	0.02
	4 cameras	0.945	0.920	0.02	0.03
	GoPro <sup>®</sup>	0.967	0.904	0.03	0.03
knee	8 cameras	0.989	0.998	0.04	0.02
	4 cameras	0.989	0.990	0.03	0.02
	GoPro <sup>®</sup>	0.974	0.918	0.02	0.03
ankle	8 cameras	0.999	0.994	0.03	0.03
	4 cameras	0.999	0.996	0.03	0.02
	GoPro <sup>®</sup>	0.995	0.989	0.04	0.03

**Table A.13:** Joint centers of Volleyball

Joint	Camera No.	Joint centers			
		correlation		SD	
		left	right	left	right
shoulder	8 cameras	0.188	0.994	0.09	0.08
	4 cameras	0.147	0.975	0.09	0.07
	GoPro <sup>®</sup>	0.138	0.983	0.09	0.08
elbow	8 cameras	0.996	0.959	0.01	0.04
	4 cameras	0.995	0.954	0.02	0.05
	GoPro <sup>®</sup>	0.992	0.912	0.02	0.08
hip	8 cameras	0.835	0.988	0.04	0.03
	4 cameras	0.740	0.984	0.04	0.03
	GoPro <sup>®</sup>	0.956	0.993	0.02	0.03
knee	8 cameras	0.992	0.999	0.01	0.02
	4 cameras	0.998	0.962	0.00	0.03
	GoPro <sup>®</sup>	0.960	0.999	0.01	0.03
ankle	8 cameras	0.359	0.999	0.01	0.02
	4 cameras	0.809	0.996	0.01	0.03
	GoPro <sup>®</sup>	0.444	0.999	0.02	0.01

**Table A.14:** Joint centers of Handball

Joint	Camera No.	Joint centers			
		correlation		SD	
		left	right	left	right
shoulder	8 cameras	0.953	0.999	0.03	0.01
	4 cameras	0.948	0.983	0.03	0.02
	GoPro <sup>®</sup>	0.934	0.993	0.04	0.03
elbow	8 cameras	0.995	0.985	0.07	0.05
	4 cameras	0.995	0.978	0.03	0.03
	GoPro <sup>®</sup>	0.978	0.986	0.02	0.03
hip	8 cameras	0.987	0.992	0.02	0.01
	4 cameras	0.996	0.978	0.02	0.02
	GoPro <sup>®</sup>	0.969	0.971	0.04	0.02
knee	8 cameras	0.998	0.991	0.02	0.01
	4 cameras	0.997	0.996	0.03	0.01
	GoPro <sup>®</sup>	0.983	0.992	0.04	0.03
ankle	8 cameras	0.992	0.993	0.02	0.01
	4 cameras	0.984	0.988	0.02	0.01
	GoPro <sup>®</sup>	0.980	0.995	0.02	0.01

Table A.15: Joint centers of Basketball

Joint	Camera No.	Joint centers			
		correlation		SD	
		left	right	left	right
shoulder	8 cameras	0.712	0.970	0.05	0.05
	4 cameras	0.695	0.957	0.05	0.04
	GoPro <sup>®</sup>	0.688	0.957	0.05	0.06
elbow	8 cameras	0.988	0.980	0.04	0.04
	4 cameras	0.990	0.976	0.03	0.03
	GoPro <sup>®</sup>	0.982	0.960	0.03	0.06
hip	8 cameras	0.913	0.960	0.03	0.02
	4 cameras	0.894	0.961	0.03	0.02
	GoPro <sup>®</sup>	0.964	0.956	0.03	0.03
knee	8 cameras	0.993	0.996	0.02	0.02
	4 cameras	0.995	0.982	0.02	0.02
	GoPro <sup>®</sup>	0.972	0.970	0.02	0.03
ankle	8 cameras	0.783	0.996	0.02	0.02
	4 cameras	0.931	0.993	0.02	0.02
	GoPro <sup>®</sup>	0.806	0.995	0.03	0.02

Table A.16: Joint centers: Average over all movements

Segment	Camera No.	Segment velocity correlation		Segment acceleration correlation	
		left	right	left	right
upper arm	8 cameras	0.905	0.801	0.709	0.820
	4 cameras	0.938	0.747	0.711	0.766
	GoPro <sup>®</sup>	0.860	0.723	0.599	0.280
lower arm	8 cameras	0.980	0.837	0.620	0.822
	4 cameras	0.916	0.875	0.521	0.741
	GoPro <sup>®</sup>	0.841	0.601	0.244	0.662
upper leg	8 cameras	0.737	0.949	0.410	0.839
	4 cameras	0.820	0.947	0.637	0.844
	GoPro <sup>®</sup>	0.688	0.896	0.396	0.647
lower leg	8 cameras	0.839	0.973	0.810	0.943
	4 cameras	0.837	0.978	0.912	0.967
	GoPro <sup>®</sup>	0.679	0.847	0.686	0.732
COM	8 cameras	0,858		0,710	
	4 cameras	0,917		0,799	
	GoPro <sup>®</sup>	0,721		0,496	
Torso	8 cameras	0,863		0,773	
	4 cameras	0,923		0,812	
	GoPro <sup>®</sup>	0,781		0,456	

**Table A.17:** Segment velocity and acceleration of Volleyball

Segment	Camera No.	Segment velocity correlation		Segment acceleration correlation	
		left	right	left	right
upper arm	8 cameras	0.938	0.957	0.744	0.929
	4 cameras	0.933	0.984	0.338	0.941
	GoPro <sup>®</sup>	0.843	0.873	0.576	0.713
lower arm	8 cameras	0.826	0.988	0.901	0.919
	4 cameras	0.892	0.983	0.870	0.910
	GoPro <sup>®</sup>	0.821	0.940	0.711	0.740
upper leg	8 cameras	0.844	0.880	0.556	0.622
	4 cameras	0.838	0.717	0.525	0.580
	GoPro <sup>®</sup>	0.553	0.777	0.189	0.282
lower leg	8 cameras	0.908	0.696	0.634	0.257
	4 cameras	0.926	0.762	0.731	0.420
	GoPro <sup>®</sup>	0.877	0.944	0.522	0.829
COM	8 cameras	0,961		0,587	
	4 cameras	0,917		0,553	
	GoPro <sup>®</sup>	0,941		0,179	
Torso	8 cameras	0,929		0,428	
	4 cameras	0,892		0,297	
	GoPro <sup>®</sup>	0,931		0,213	

**Table A.18:** Segment velocity and acceleration of Handball

Segment	Camera No.	Segment velocity correlation		Segment acceleration correlation	
		left	right	left	right
upper arm	8 cameras	0.915	0.954	0.860	0.913
	4 cameras	0.958	0.935	0.874	0.892
	GoPro <sup>®</sup>	0.942	0.855	0.794	0.545
lower arm	8 cameras	0.930	0.954	0.853	0.829
	4 cameras	0.952	0.913	0.855	0.882
	GoPro <sup>®</sup>	0.878	0.956	0.780	0.673
upper leg	8 cameras	0.934	0.902	0.845	0.847
	4 cameras	0.832	0.956	0.829	0.913
	GoPro <sup>®</sup>	0.862	0.842	0.690	0.729
lower leg	8 cameras	0.978	0.930	0.852	0.873
	4 cameras	0.925	0.956	0.827	0.882
	GoPro <sup>®</sup>	0.912	0.887	0.748	0.729
COM	8 cameras	0,960		0,924	
	4 cameras	0,925		0,913	
	GoPro <sup>®</sup>	0,967		0,818	
Torso	8 cameras	0,953		0,933	
	4 cameras	0,919		0,891	
	GoPro <sup>®</sup>	0,949		0,797	

**Table A.19:** Segment velocity and acceleration of Basketball

Segment	Camera No.	Segment velocity correlation		Segment acceleration correlation	
		left	right	left	right
upper arm	8 cameras	0.919	0.904	0.771	0.887
	4 cameras	0.943	0.889	0.641	0.866
	GoPro <sup>®</sup>	0.882	0.817	0.656	0.513
lower arm	8 cameras	0.912	0.926	0.792	0.856
	4 cameras	0.920	0.924	0.749	0.844
	GoPro <sup>®</sup>	0.847	0.832	0.578	0.692
upper leg	8 cameras	0.838	0.910	0.603	0.769
	4 cameras	0.830	0.874	0.664	0.779
	GoPro <sup>®</sup>	0.701	0.838	0.425	0.552
lower leg	8 cameras	0.908	0.866	0.766	0.691
	4 cameras	0.896	0.899	0.823	0.756
	GoPro <sup>®</sup>	0.823	0.893	0.652	0.763
COM	8 cameras	0,926		0,740	
	4 cameras	0,920		0,755	
	GoPro <sup>®</sup>	0,876		0,498	
Torso	8 cameras	0,915		0,711	
	4 cameras	0,911		0,667	
	GoPro <sup>®</sup>	0,887		0,488	

**Table A.20:** Average over all movements of segment velocity and acceleration